Two JET waveforms which make the difference*

Leonid E. Zakharov(PPPL)

in collaboration with

Sergei Gerasimov, JET Contributors[1] (CCFE, UK) and Xujing Li (ICM&SEC, China)

[1]See the Appendix of F. Romanelli et al., Proceedings of the 25th IAEA Fusion Energy Conference 2014, Saint Petersburg, Russia

NSTX-U Physics Meeting
January 12, 2015, Princeton NJ

*This work is partially supported by US DoE contract No. DE-AC02-09-CH11466, by the Chinese National Magnetic Confinement Fusion Science Program 2011GB105003, and has been carried out within the framework of the EUROfusion Consortium and has received funding from the Euratom research and training programme 2014-2018 under grant agreement No 633053 and from the RCUK Energy Programme [grant number EP/I501045].

PPPL PRINCETON PLASMA PHYSICS LABORATORY

Abstract

The talk presents the theory, simulations and physics of VDEs, consistent with JET measurements of toroidal asymmetries in the plasma current and toroidal magnetic field flux (diamagnetic signal). In 2007, the Tokamak MHD theory introduced the Hiro currents and gave the explanation of the wall currents in JET (still called the "halo" currents, despite their opposite direction to measurements). Now, the JET data on diamagnetic signals support the explanation of the currents to the tiles surface, discovered earlier on DIII-D in VDEs and measured on many tokamaks, by the theory introduced Evans currents, while being in conflict with the conventional "halo"-current interpretation.

The formulated understanding of VDE, which excludes the halo-currents as the players, opens new approaches for measurements, numerical simulations, and deeper theory development for prediction of the disruption effects in ITER.

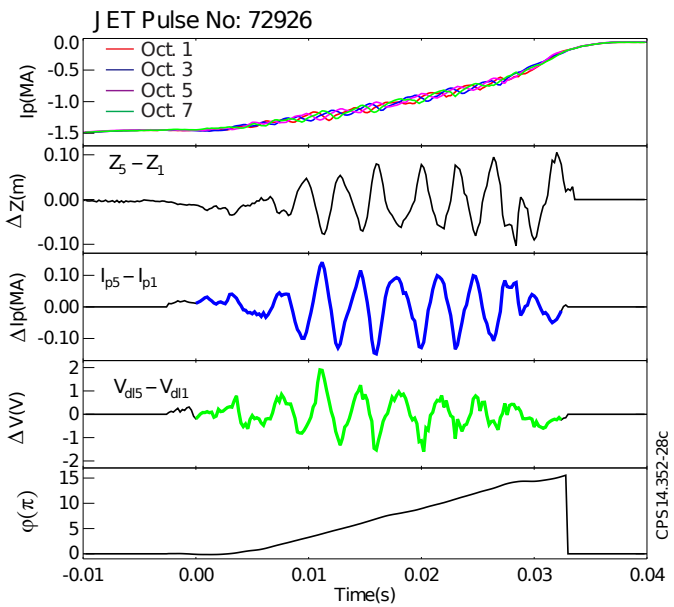

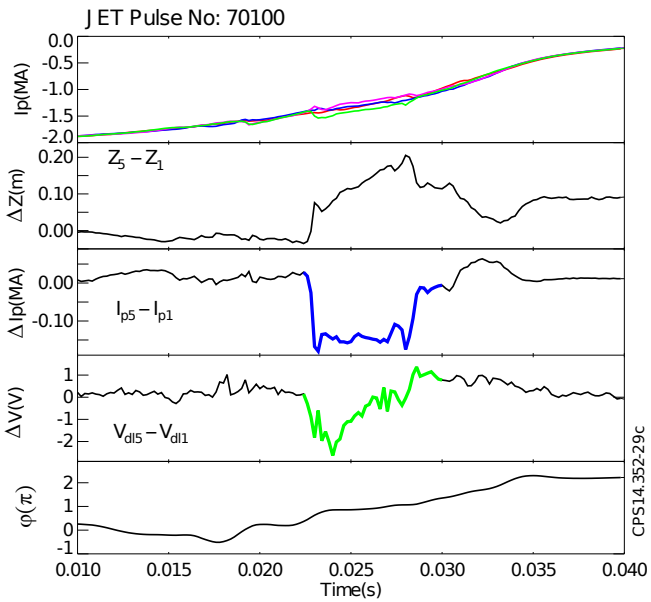

Contents

1 Attached poloidal currents on DIII-D (1991) 4
2 Overview of theory. VDE and fast equilibrium evolution 6
  2.1 The δ-functional surface current model . . . 8
  2.2 Toroidal Hiro currents along plasma facing surface . . . 9
  2.3 Beyond the $\delta-$functional current model . . . 12
  2.4 Xiong tiles on EAST . . . 14
  2.5 VDE as a current and voltage generator . . . 16
3 JET VDEs. Wall Touching Kink Mode 1/1 17
  3.1 Large VDE on JET (Aug.10,1996, 16:54:12, #38070) . . . 22
  3.2 JET asymmetry in the Diamagnetic signal . . . 25
4 Tokamak MHD (TMHD) 30
5 The VDE-code for EAST to be a research tool 34
  5.1 The real in-vessel geometry is an essential part . . . 36
  5.2 Free-boundary equilibria with ESC-EEC . . . 37
  5.3 VDE simulations motivate innovative diagnostics . . . 38
6 Summary 40

1 Attached poloidal currents on DIII-D (1991)

E.J. STRAIT, L.L. LAO, J.L. LUXON, E.E. REIS. "Observation of poloidal current flow to the vacuum vessel wall during vertical instabilities in the DIII-D tokamak", Nucl. Fusion v. 31 p. 527 (1991)

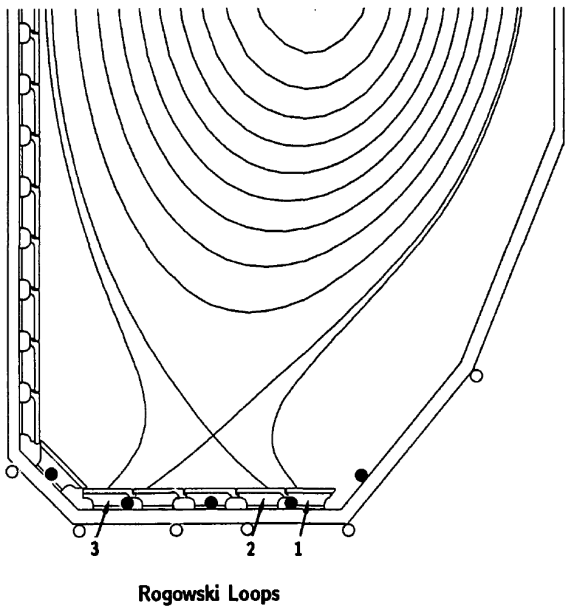

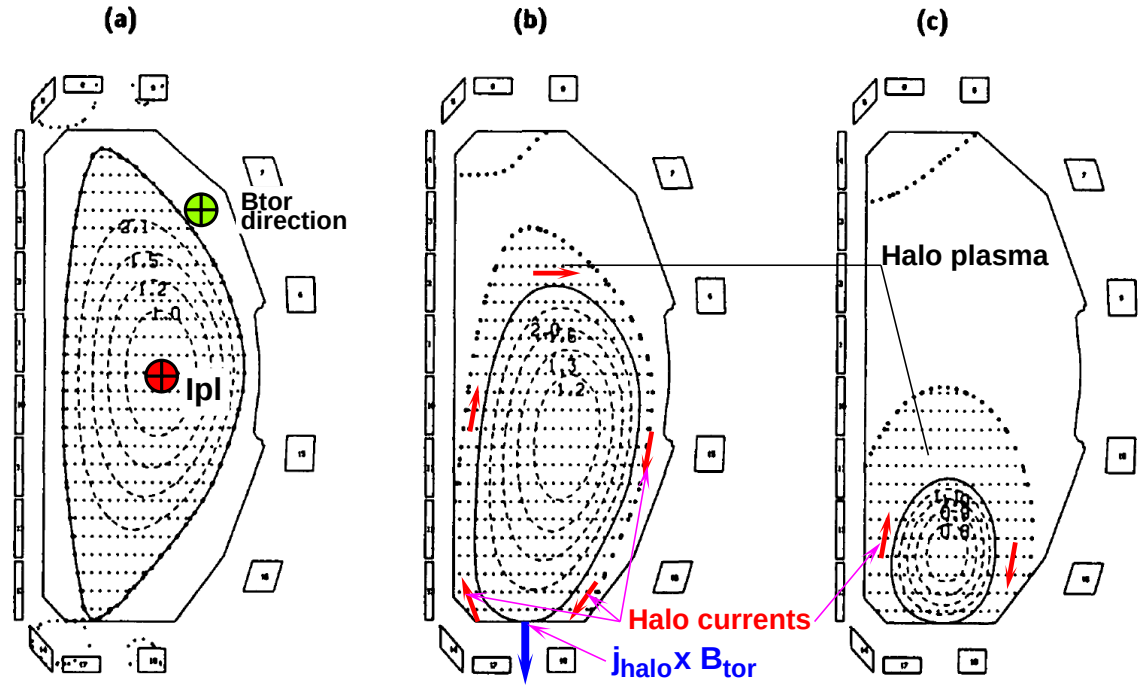

FIG. 3. Equilibrium flux plots from EFIT at three times during the vertical instability: (a) 2660 ms, (b) 2675 ms and (c) 2684 ms. Plasma current was allowed in the hatched region, including part of the SOL.

Large "halo" currents to tiles discovered far away from the last closed magnetic surface:

- ***Generated by EMF*** $-d(LI_{pl})/dt$ ***in the direction of plasma current due to plasma shrinking***
- ***Force-free in the halo zone***
- ***Flow along a short path in the wall across*** B_{tor} ***and exert a large vertical force to the wall***
- ***Balance the plasma vertically***

Driving voltage (EMF) for halo currents

6. DISCUSSION

The attached current measured by the armour tile Rogowski loops in the early stages of the vertical instability is probably driven by the vertical motion of the plasma. After the discharge comes into contact with the vacuum vessel wall during its downward motion, the cross-sectional area of the plasma begins to decrease (see Fig. 3). According to Lenz's law, the contraction of the plasma boundary across the toroidal magnetic field should induce a poloidal current which tends to conserve toroidal flux within the conducting plasma. The toroidal field points out of the page in Figs 1 and 3, so the sign of the observed current is consistent with this prediction. In the present example, the cross-sectional area decreases at a fairly constant rate of about 100-120 m^2/s in a toroidal field of 1.1 T, which, according to Faraday's law, would generate a poloidal electromagnetic force (EMF) of 110-130 V. The total toroidal flux contained in the discharge before the instability, about 2 Wb, can drive a much larger time integrated poloidal current (and hence a larger impulse to the vessel) than the diamagnetic flux of about 0.03 Wb.

From E.J. Strait et al, NF (1991)

The statement in blue is incorrect.

$$U_{pol} \simeq -\frac{\partial \Phi}{\partial t} \simeq 0.$$

There is only a toroidal (in fact along $\vec{B}$) EMF,

$$U_{tor} = U_{voltage}^{loop} \simeq -\frac{\partial \Psi^{edge}}{\partial t}$$

due to poloidal flux conservation.

It tries to preserve the plasma current when the plasma cross-section shrinks.

It is right to neglect plasma inertia and consider only the equilibrium evolution

$$\tau_{MHD} \simeq \frac{R}{V_A} = \underbrace{\frac{R}{2.18 \cdot 10^6 B/\sqrt{n}}}_{<1\ \mu s} \ll \underbrace{\tau_{VDE}}_{\simeq 1\ ms} \ll \underbrace{\tau_{transport}}_{\simeq 0.1\ s} \ll \underbrace{\tau_{resistive}}_{\simeq 1\ s} \qquad (2.1)$$

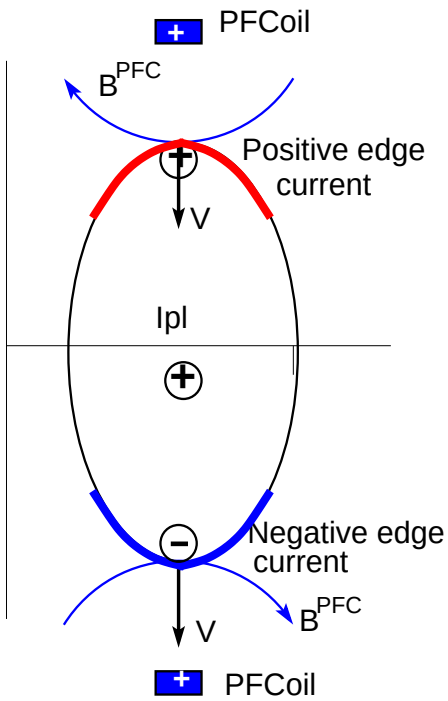

But

This is a SPECIAL, fast equilibrium evolution, which preserves the magnetic fluxes

Localized currents are automatically generated at the plasma surface (edge)

- ***negative (opposite to the plasma current) at the leading side***
- ***positive at the trailing side***

$$-\frac{\partial \vec{A}^{i,surf}}{\partial t} \underbrace{-\frac{\partial \vec{A}^{pl,core}}{\partial t} + V B_{pl} \vec{e}_\varphi}_{vanishes\ for\ m/n=1/0} + \underbrace{\vec{V} \times \vec{B}^{PFC}}_{Driving\ EMF} - \nabla \phi_E^{surf} = \frac{\vec{j}}{\sigma} \qquad (2.2)$$

Surface currents in tokamaks

The generation of the surface (edge) currents is the fundamental tokamak MHD effect

Plasma electrons preserve the alignment of the plasma surface with the magnetic field

$$(\vec{B} \cdot \nabla \sigma_{\|}) \simeq (\vec{B} \cdot \nabla T_e) \simeq 0, B_{normal} \simeq 0$$

- ***Without them the tokamak plasma would not exist - it would be always unstable***
- ***It is a fundamental effect of the real plasma - the plasma"resistivity" determines only the thickness of the current layer.***
- ***The perturbed plasma generates the same value of the edge current independent of plasma resistivity - works as a current generator***

The simple, δ-functional model of the surface (edge) currents is perfect to predict the most robust MHD effects in the tokamak plasma

They are not based on the fictitious theoretical model of "ideal conductivity"

2.1 The δ-functional surface current model

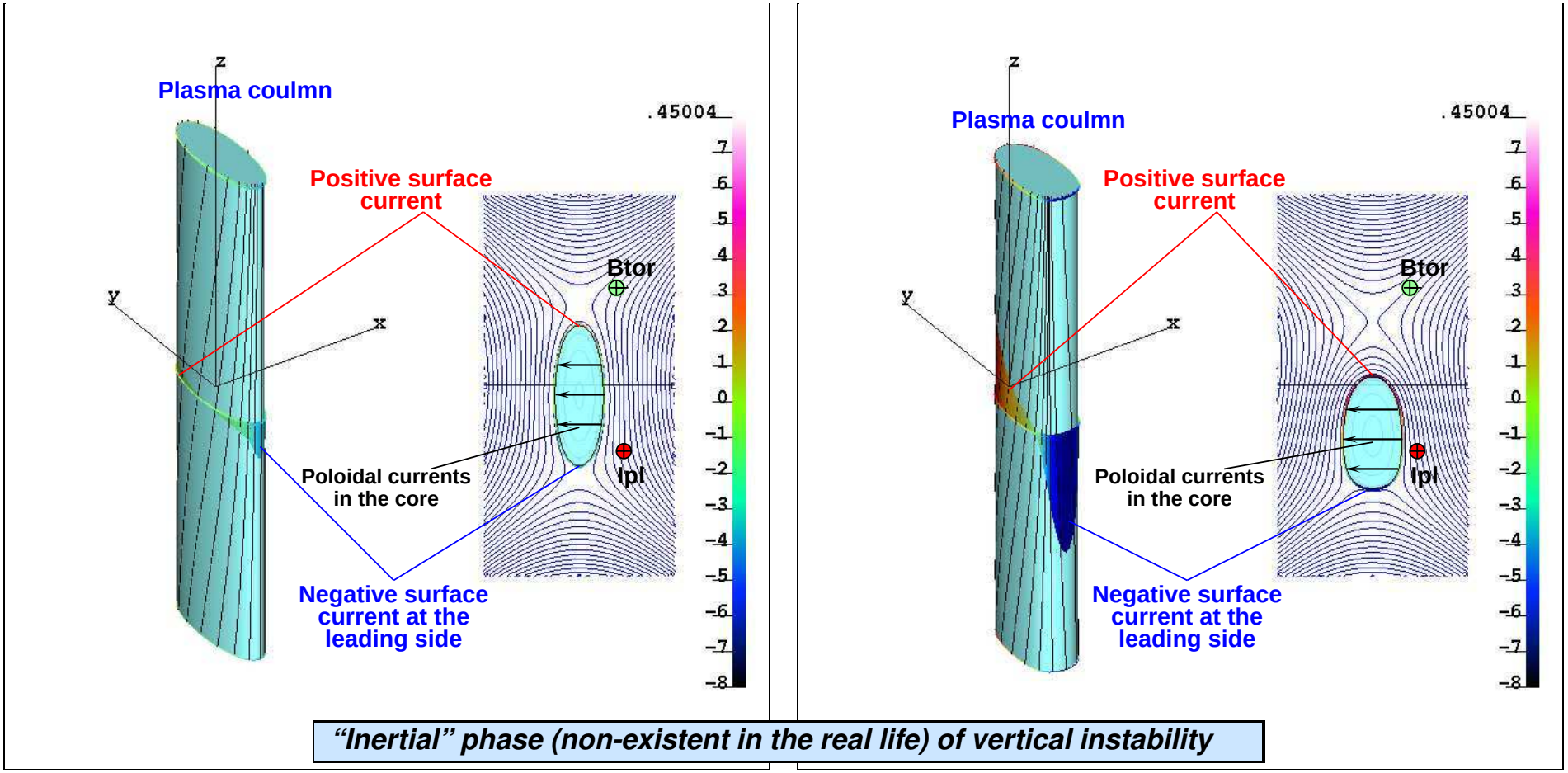

"Inertial" phase (non-existent in the real life) of vertical instability

1. *Equilibrium in the core with flux conservation determines the distribution of surface currents.*
2. $\oint(\vec{\imath}\times\vec{B}_{pol})dS \;\propto\; \delta z_{pl} I_{pl}\vec{e}_z$ *force is applied to the surface currents* $\vec{\imath}$ *in the direction of* δz_{pl}
3. *Weak poloidal currents* $\vec{\jmath}_{pol} = (\nabla\tilde{F}\times\vec{e}_z)$*, are generated in the core. They enter the plasma edge and make the surface currents force-free.*
4. *The* $(\vec{\jmath}_{pol}\times\vec{B}_{tor})$ *force in the core is compensated by plasma inertia. It advances the plasma shape.*

2.2 Toroidal Hiro currents along plasma facing surface

On the way to the wall, the plasma faces the tiles

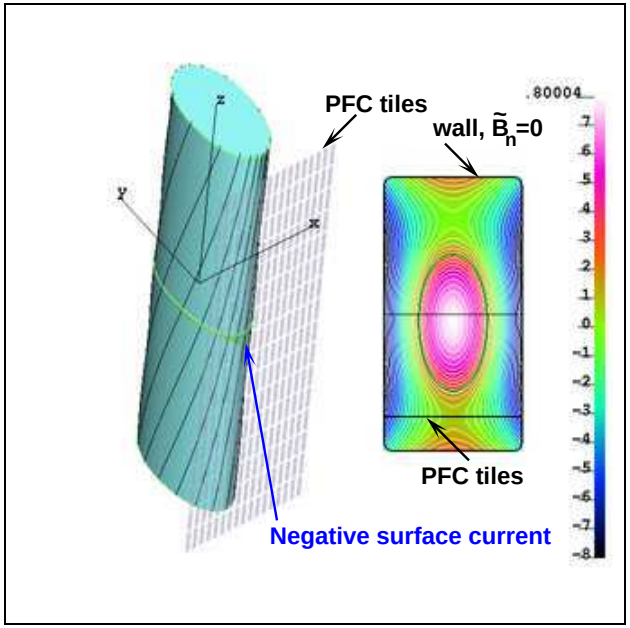

Initial plasma displacement

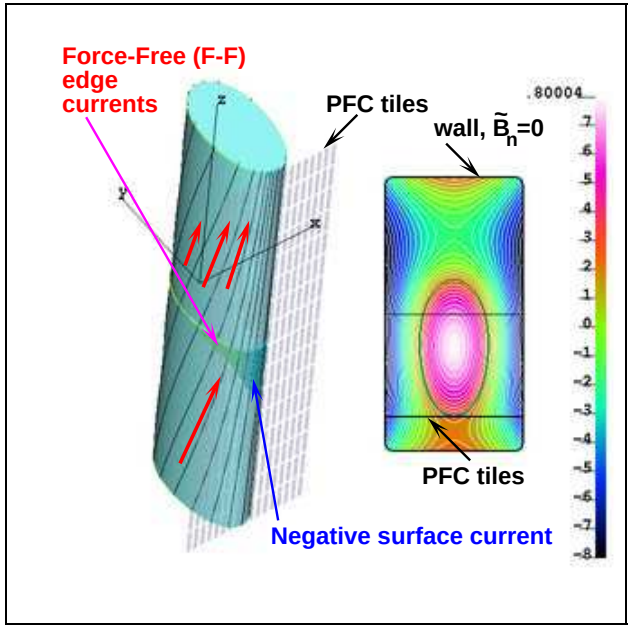

Negative surface current at the leading edge

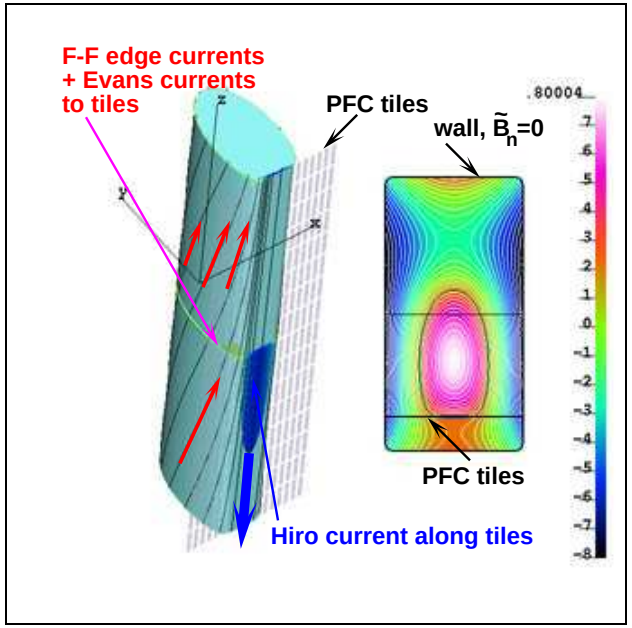

Hiro, Evans currents, formation of two Y-points

Predicted by the TMHD theory
(a) surface currents at the plasma boundary
(b) Hiro currents along the tile surface in the toroidal direction
(c) Evans currents from the plasma edge to the tile surface are well reproduced by the new VDE code.

Intermediate equilibrium maintained by the Hiro currents

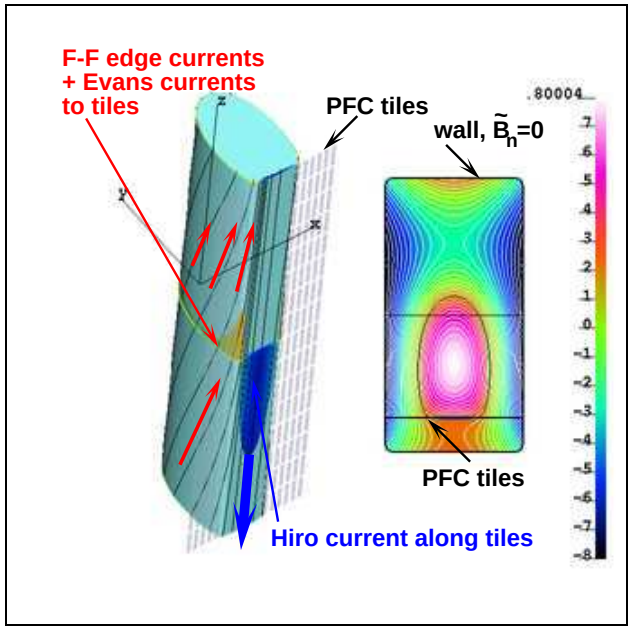

Hiro currents apply the force to tiles

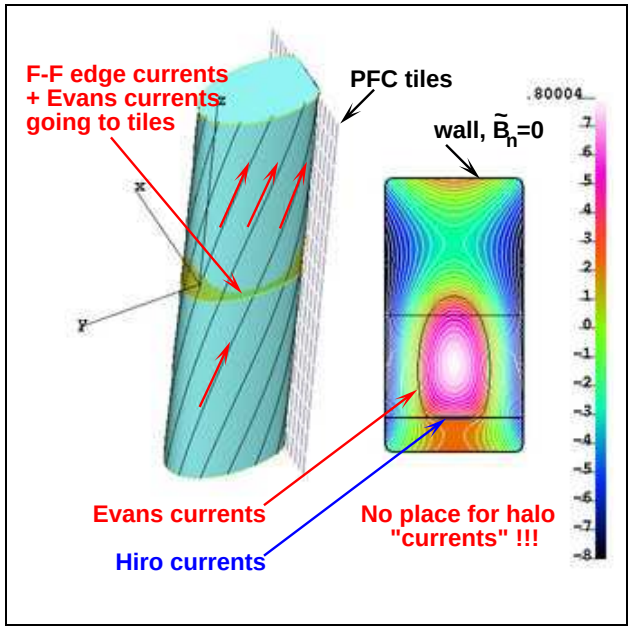

Evans currents. No place for fake "halo" currents

Plasma shrinking due to decay of Hiro currents

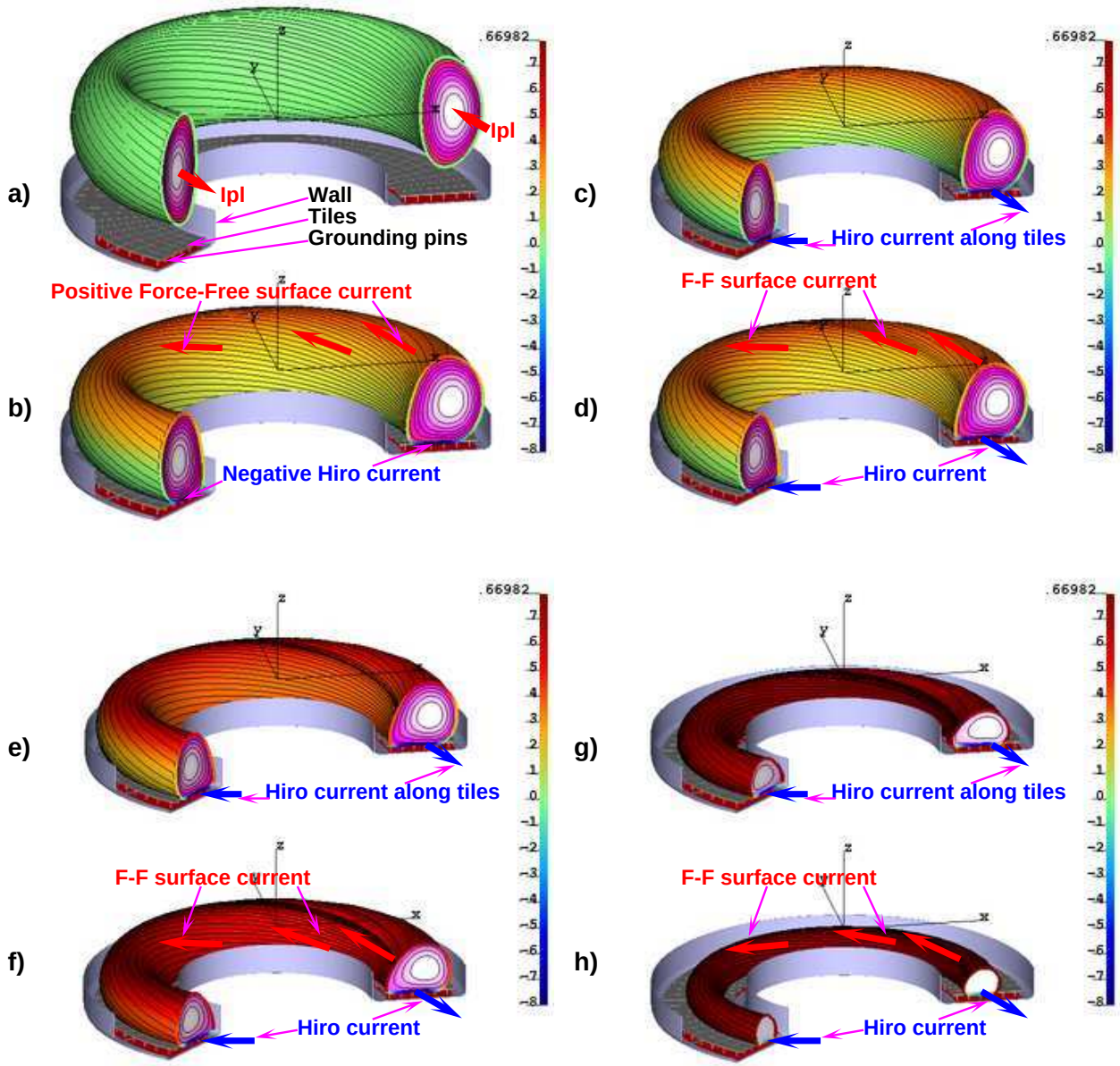

During plasma shrinking I_{pl} decays

This generates an additional poloidally symmetric compensation current at the plasma edge

At later stage its contribution enhances the darkness of the color of the total F-F edge current

On the way, the kink mode m/n=1/1 will be developed

2.3 Beyond the $\delta-$functional current model

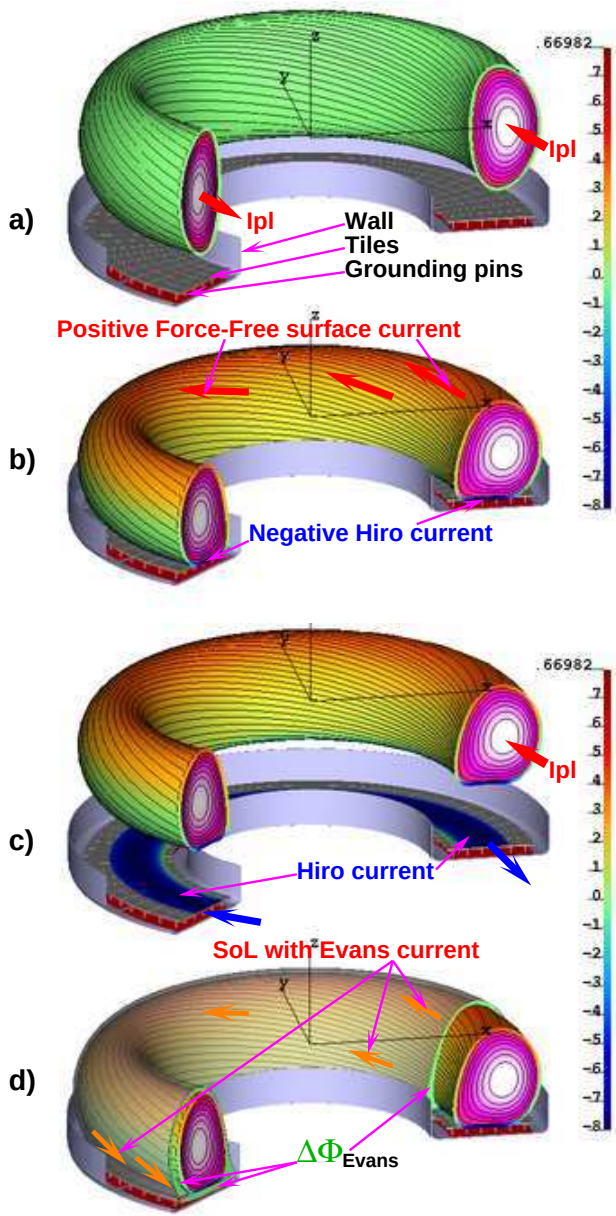

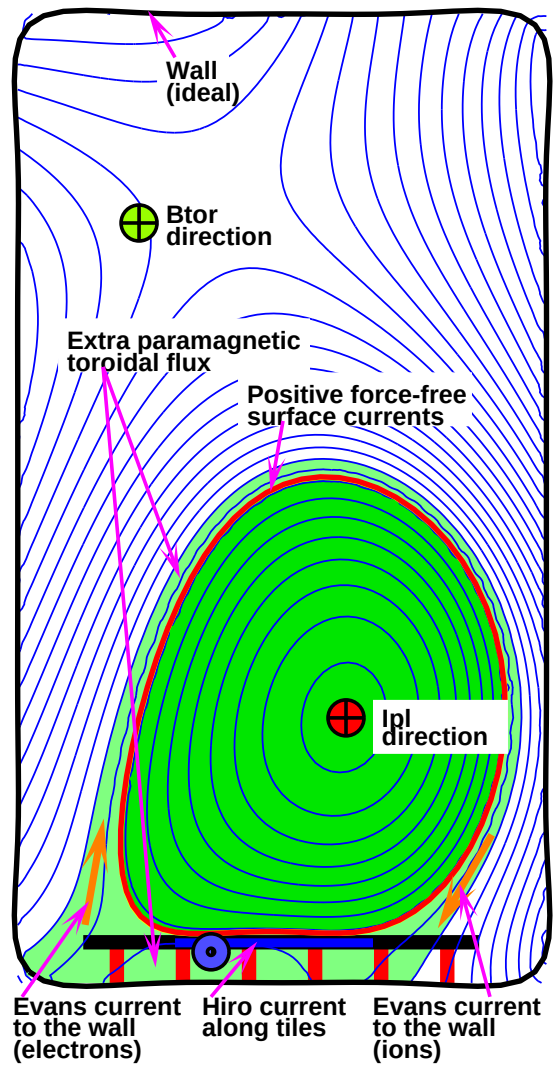

Resistive thickness of the F-F currents

$$\Delta^{FF} \simeq 2\sqrt{\frac{t}{\mu_0\sigma_{\|}}} \simeq \frac{2\sqrt{t_s}}{7T_{keV}^{3/4}}$$

The shrinking plasma core releases the plasma particles and creates the halo zone

The Evans currents in the halo zone are a fraction of F-F currents, and are limited by

$$I_{pol}^{Evans} < 2e\frac{dN_e}{dt}$$

The Evans currents to the tiles surface are driven by the loop voltage and observed as the currents to the tiles surface

There is no place for other "halo" currents

The Evans currents are the side effect of MHD instability

Edge voltage and thickness of the edge F-F currents

Total Force-Free surface current I^{F-F}

$$I^{F-F} \simeq |I^{Hiro}| = \oint i^{F-F} dl, \quad i^{F-F} \simeq \frac{I^{Hiro}}{L_{pol}} \simeq \frac{I^{Hiro}}{2\pi a_{pl}}. \tag{2.3}$$

Diffusion of an initially δ***-functional edge current into the plasma core***

$$j^{edge}(a,t)|_{t=0} = i^{F-F} \cdot \delta(a - a_{pl}),$$
$$j(a,t) = \frac{i^{F-F}}{\Delta} \cdot \frac{2}{\sqrt{\pi}} \cdot e^{-\frac{(a-a_{pl})^2}{\Delta^2}}, \qquad \Delta_m = 2\sqrt{\frac{t}{\mu_0 \sigma_{\|}}} \simeq \frac{2\sqrt{t_s}}{7T_{keV}^{3/4}}. \tag{2.4}$$

The associated resistive Voltage $U^{edge}(t)$ ***at the plasma surface*** $x = 0$

$$U^{edge}(t) = 2\pi R \cdot \frac{j^{edge}}{\sigma_{\|}} \simeq \frac{R}{a} \cdot \frac{I^{Hiro}}{\sigma_{\|}} \cdot \sqrt{\frac{\mu_0 \sigma_{\|}}{\pi t}} \simeq \frac{R}{10a} \cdot \frac{I_{MA}^{Hiro}}{T^{3/4}} \cdot \sqrt{\frac{1}{t_s}} \tag{2.5}$$

going down with time.

2.4 Xiong tiles on EAST

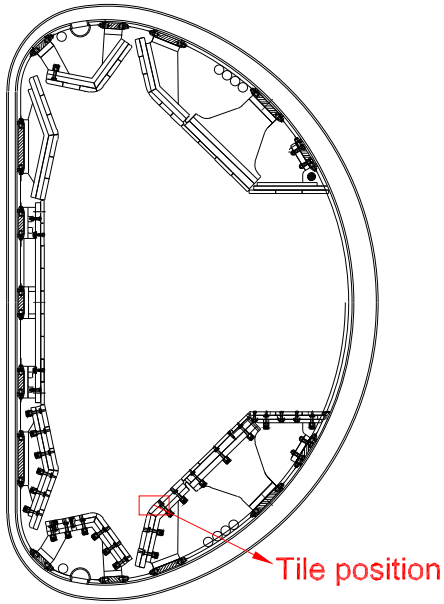

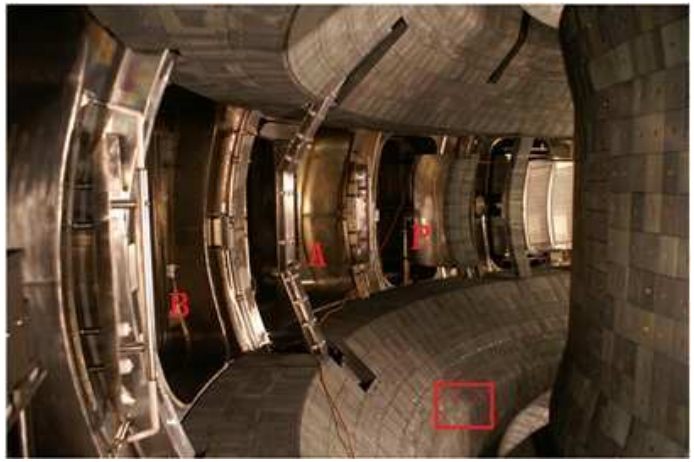

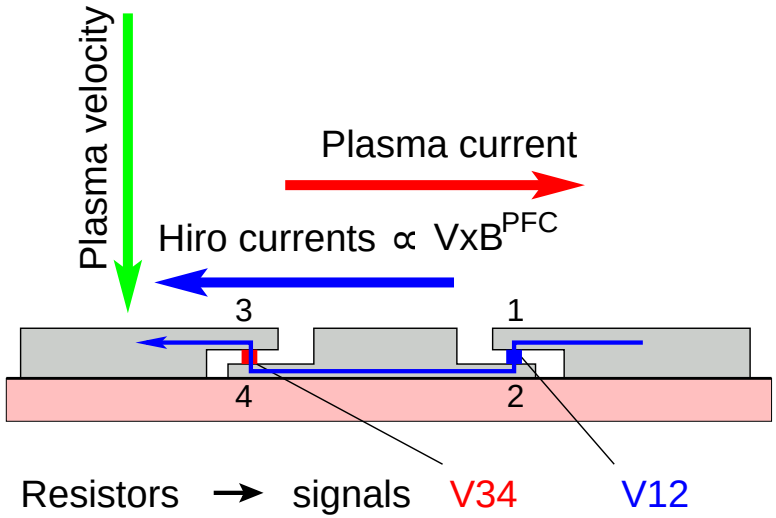

Two resistors between 3 shaped Mo tiles mounted through the thermal contact on a 2 cm thick copper heat sink plate, point-wise grounded

4 types of currents can be distinguished by the Xiong tiles.

First measurements of Hiro currents in VDE

Toroidal Hiro currents ($\simeq 0.8kA$), opposite to the plasma current, were measured on EAST in May 2012 for the first time in an axisymmetric VDE

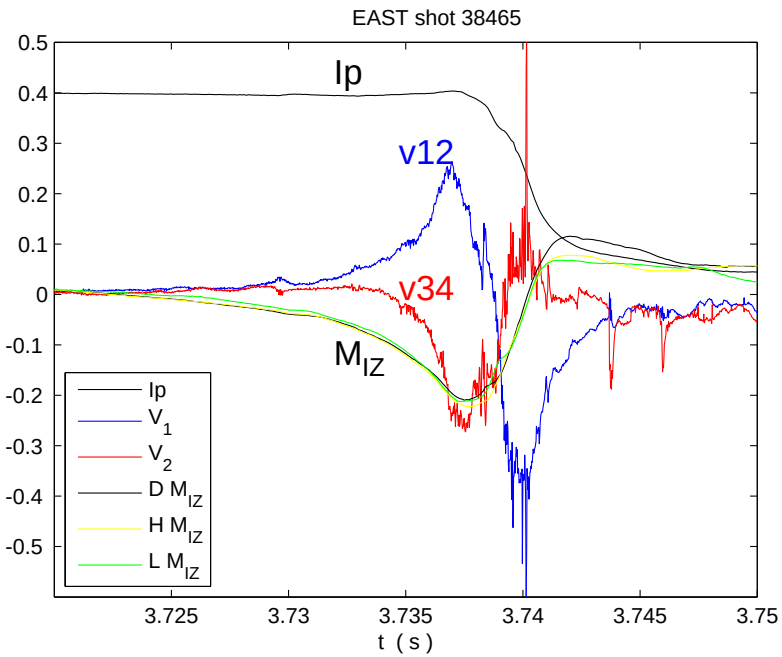

Downward VDE

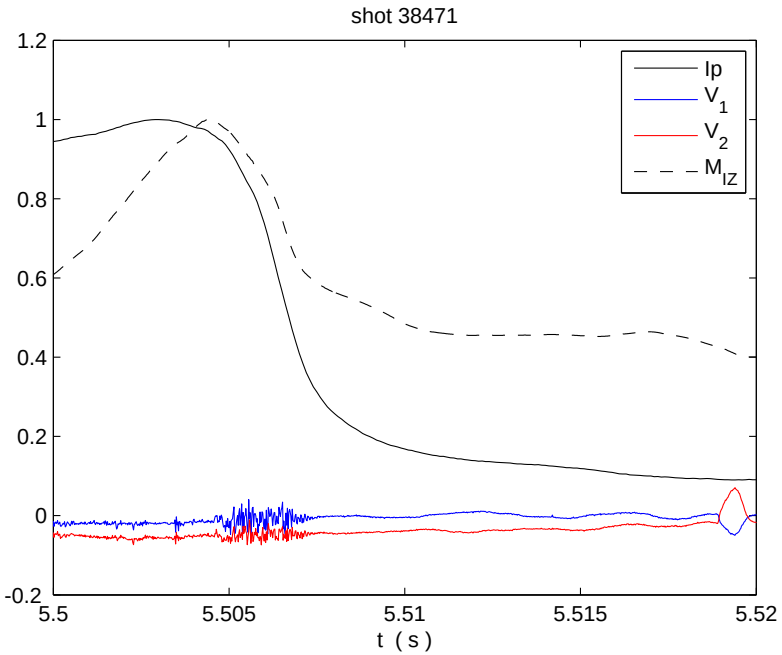

Upward VDE

No toroidal asymmetry, n=0, Ipl and Mirnov signals from three cross-sections are identical

Hiro currents in n=0 VDE are NOT SHARED between plasma and the tiles.

2.5 VDE as a current and voltage generator

1. ***VDE instability, acting as a current generator, excites***
   - (a) ***the Hiro currents in the wetting zone of the plasma facing structures, and***
   - (b) ***the Force-Free edge currents at the plasma free surface plasma surface***
   - (c) ***the resistive voltage*** $\simeq 2\pi R\sigma j^{F-F}$ ***created along the free surface***
2. ***The Hiro currents provide the plasma equilibrium and exert the forces on the vessel.***
   (All other currents are not the players in forces on the vessel)
3. ***Plasma motion into the tiles is necessary to maintain the necessary level of Hiro currents***
4. ***Shrinking plasma cross-section***
   - (a) ***releases plasma core particles and creates the "halo"-zone***
   - (b) ***creates additional loop voltage in the halo-zone from the conventional plasma current decay***
   - (c) ***releases a fraction of F-F currents to the tile surface as the Evans currents, which are measured as the tile pins currents***

The total Evans current is limited by the maximum ion saturation current

$$I_{pol}^{Evans} < 2e\frac{dN_e}{dt}, \quad N_e \equiv \int n_e dV_{olume} \tag{2.6}$$

As a reference

$$\begin{aligned} \textbf{DIII-D}: &\quad \int I^{Evans}(t)dt < 2eN_e \simeq 2\cdot 1.6\cdot 10^{-19}\cdot 3\cdot 10^{19}\cdot 20_{m^3} \simeq 200\ [A\cdot s], \\ \textbf{JET}: &\quad \int I^{Evans}(t)dt < 2eN_e \simeq 2\cdot 1.6\cdot 10^{-19}\cdot 3\cdot 10^{19}\cdot 60_{m^3} \simeq 600\ [A\cdot s] \end{aligned} \tag{2.7}$$

3 JET VDEs. Wall Touching Kink Mode 1/1

Introduced in 2007 as a key element of disruptions

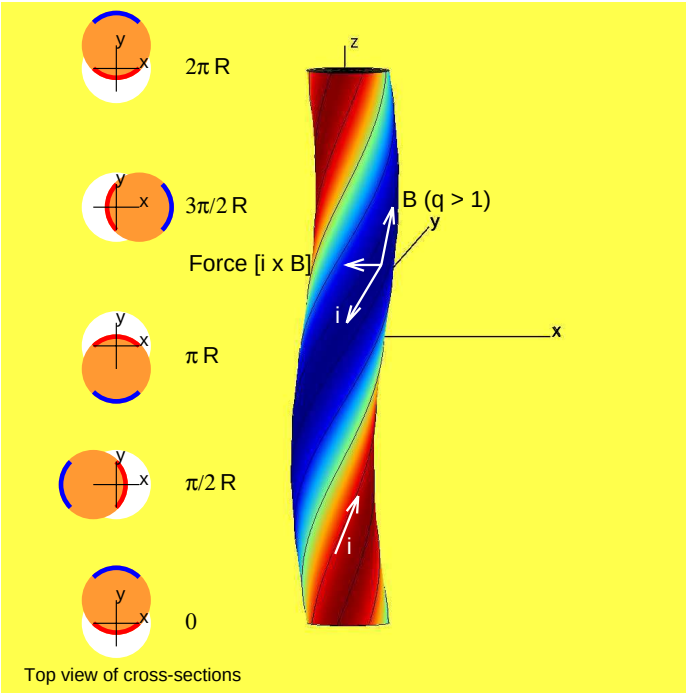

***named in the honor of Hironori Takahashi**

Only negative part of $i(\omega, \varphi)$ can be shared between plasma and the wall.

The m/n=1/1 WTKM in VDE always leads to asymmetry in plasma current measurements.

Hiro currents are predicted by theory of perturbed equilibrium

This makes the Hiro currents prediction unshakable.

Magnetic Diagnostic (1)

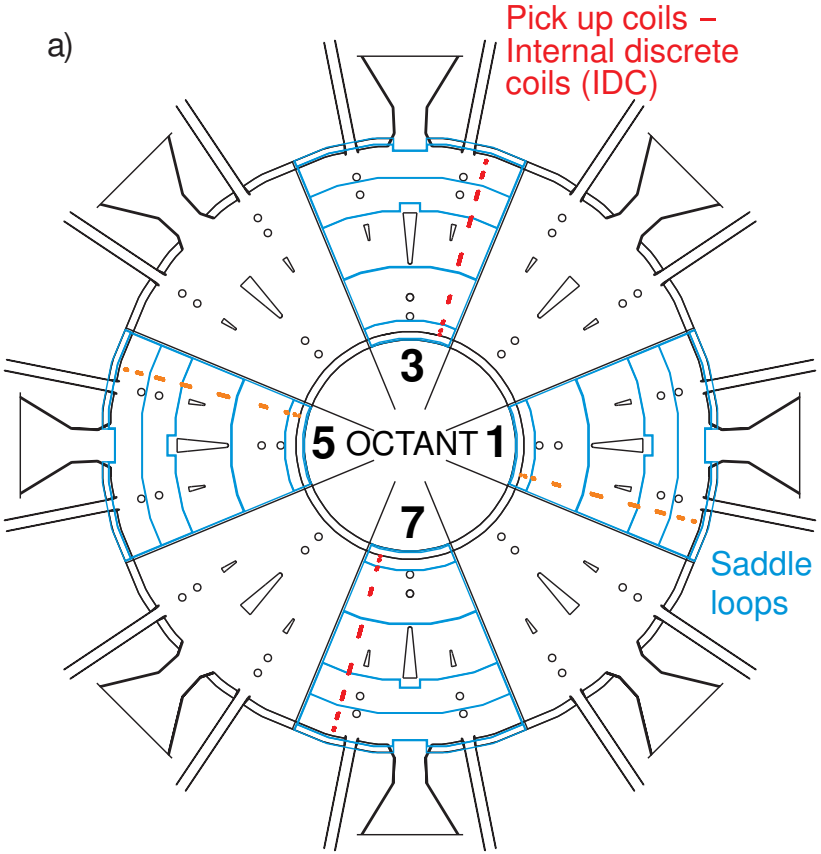

Plan view of JET vessel, showing the toroidal locations of **pick up coils** and **saddle loops**

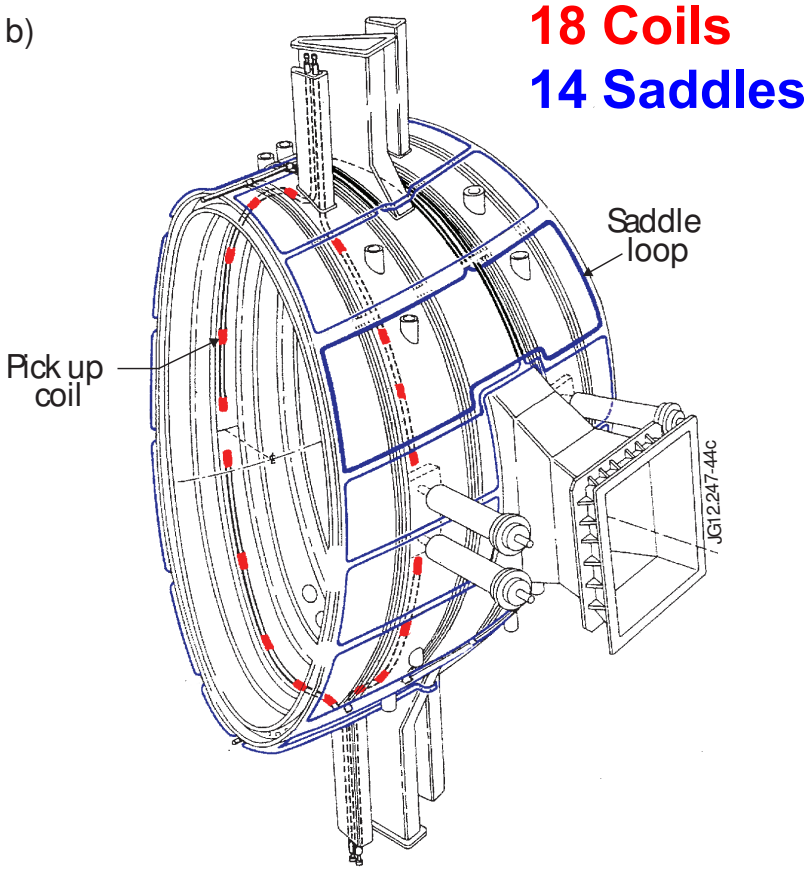

Each vessel octant was equipped with **pick up coils (IDC)** and **saddle loops**

The integrated signals are recorded regularly with 16-bit ADC at 5 kHz from 3/11/2005 onwards. *(The plasma current quench durations > 10ms)*

Magnetic Diagnostic → Current Moments

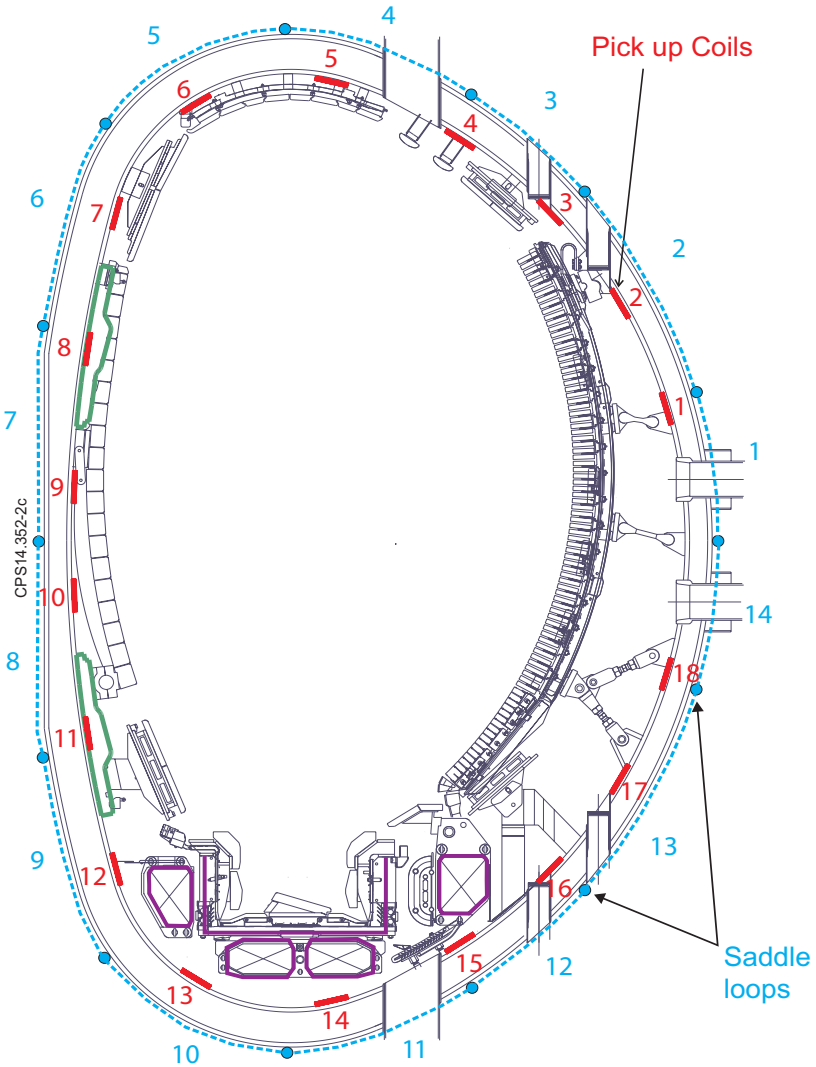

Plasma Current Calculation ⇨

$$\mu_0 I = \oint \vec{B}\,\vec{dl}$$

⇩

$$I_p = \frac{1}{\mu_0}\sum_{i=1}^{18} B_{\vartheta i} d_i - \sum_{i=1}^{4} n_{Di} I_{Di} - (I_{RRU} + I_{RRL})$$

First Plasma Current Moment Calculations ⇨

$$M_{IR} \equiv \int (R - R_o) J_\phi dR dZ$$

$$M_{IZ} \equiv \int Z J_\phi dR dZ$$

⇩

$$M_{IZ} = \frac{1}{\mu_0}\left(\sum_{i=1}^{18} B_{\vartheta i} z_i d_i + \frac{1}{2\pi}\sum_{i=1}^{14} \Psi_i \ln\left(\frac{R_o}{r_i}\right)\right) - \sum_{i=1}^{4} z_{Di} n_{Di} I_{Di} - (z_{RRU} I_{RRU} + z_{RRL} I_{RRL})$$

Divertor support structure and divertor PF coil cases are not included in calculations (~5% of Ip at disruption), because there are no reliable measurements. It does not affect the asymmetry calculation.

Magnetic Diagnostic – Diamagnetic Poloidal Loops

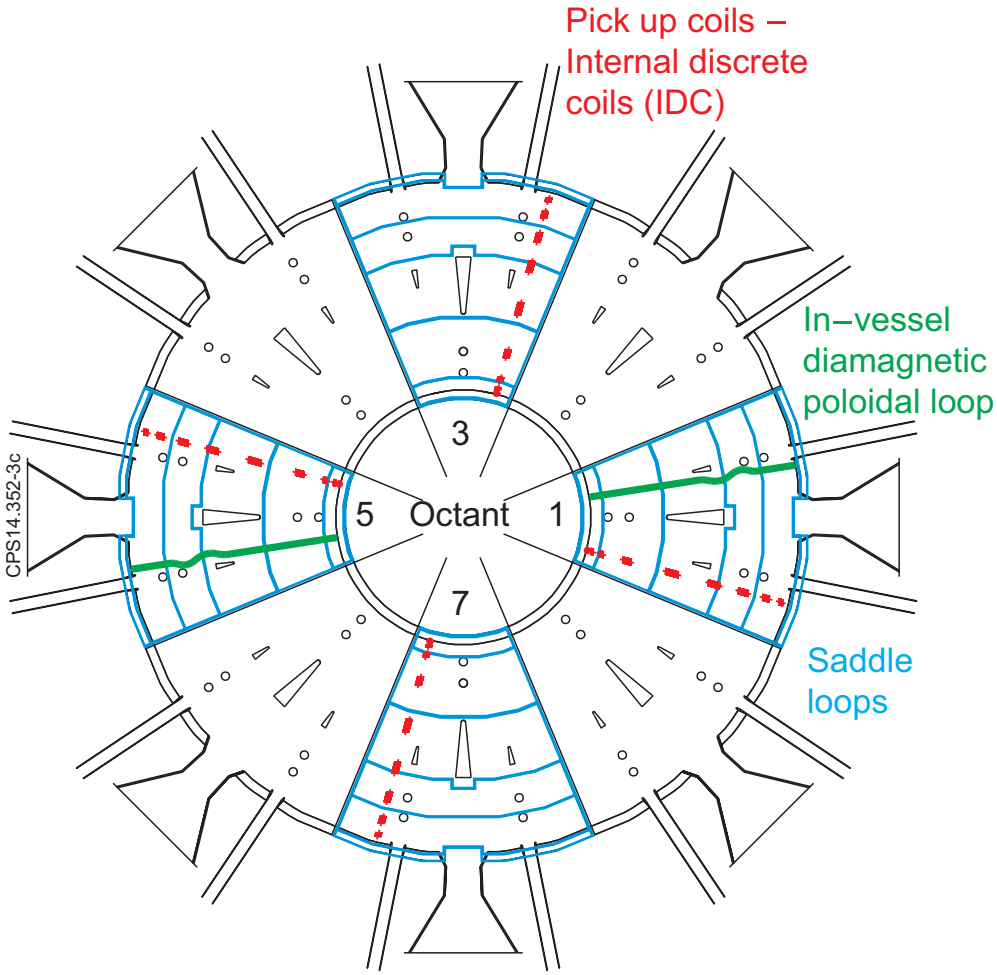

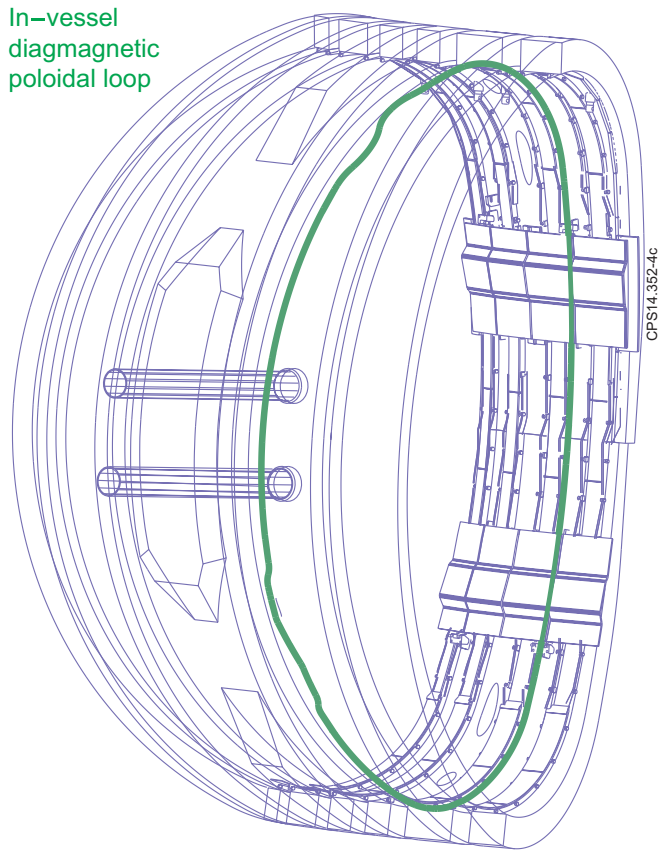

Plan view of JET vessel, showing the toroidal locations of **in-vessel diamagnetic poloidal loops**

#1 and #5 octants equipped with **in-vessel diamagnetic poloidal loops**

Radial Vessel Displacement Diagnostic

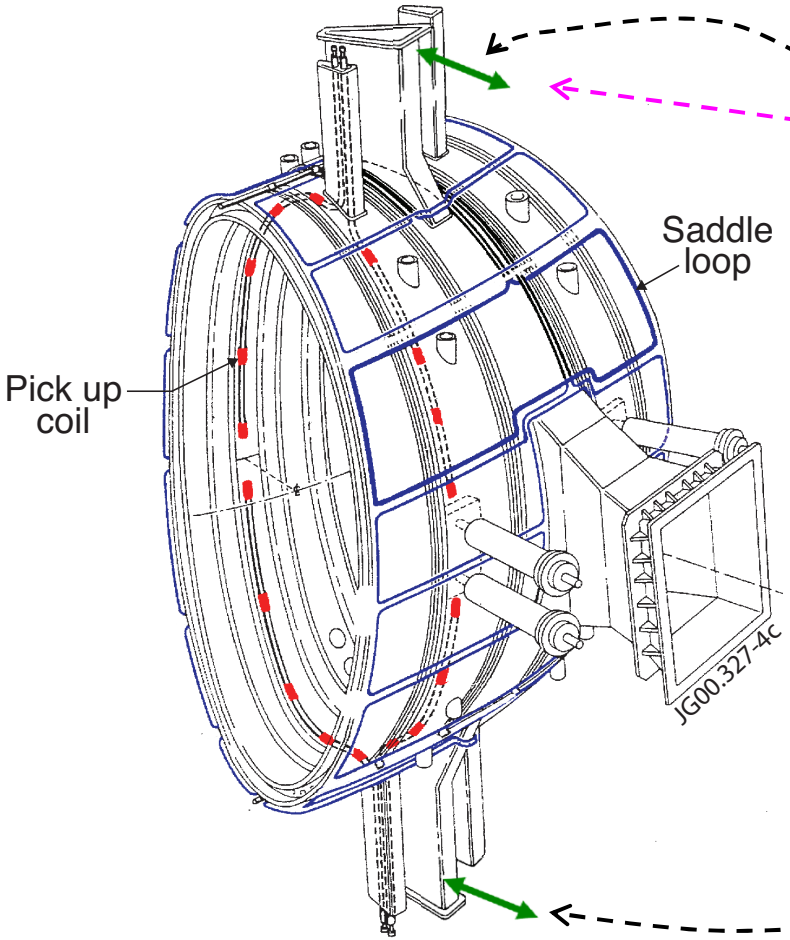

Displacement transducers

Displacement transducer

Transducers measure radial movement at vertical port of the each vessel octant with respect to mechanical structure

Vessel current during VDE, #38070

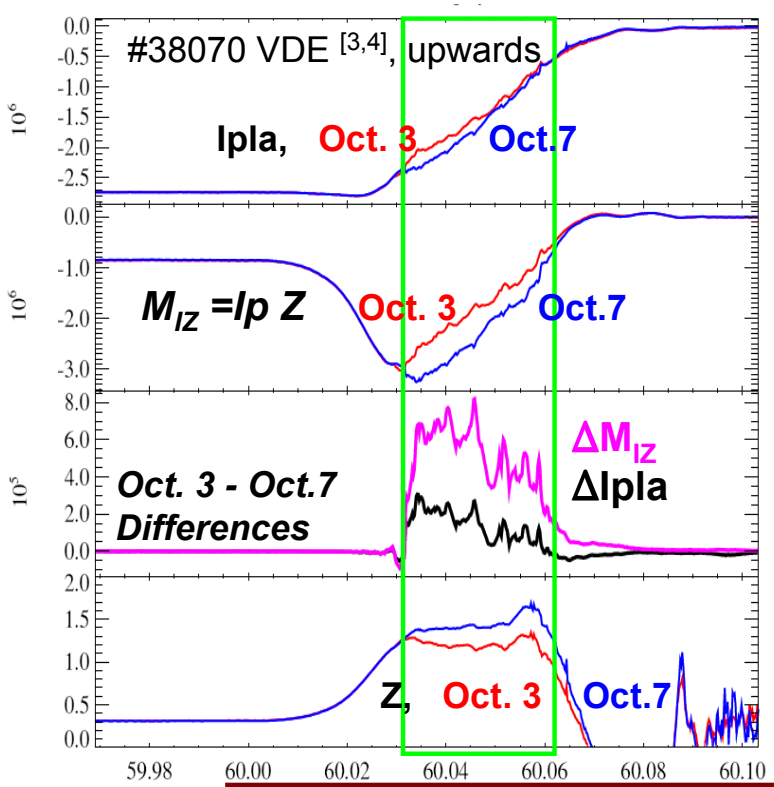

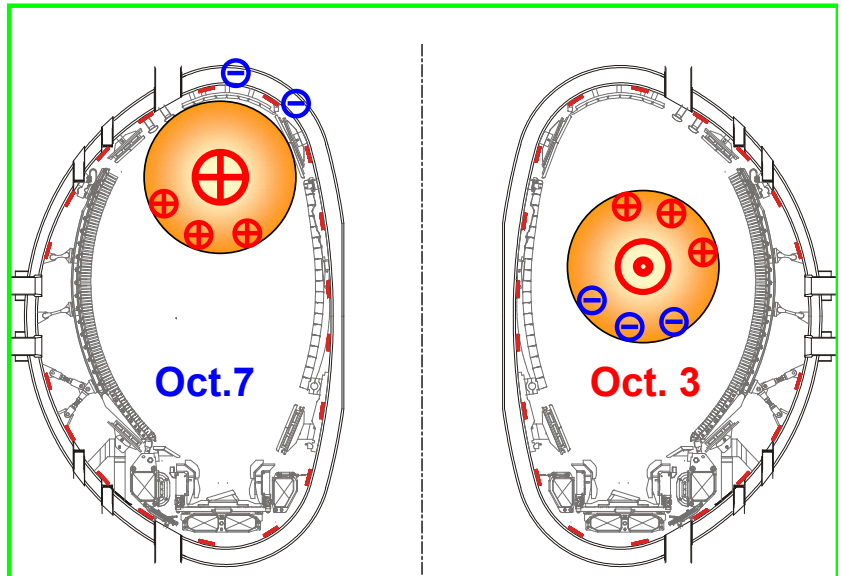

- In octant 7 the plasma is closer to top of the vessel than in octant 3.
- **The current from plasma flows on vessel in octant 7.**

The measured Ipla in octant 7 is higher then in octant 3 ➔ the missing vessel current in octant 7 is OPPOSITE to Ipla!

The "halo" current based interpretation predicts the opposite sign of asymmetry in the current measurement and contradicts JET Ipla's.

S N Gerasimov et al, Scaling JET Disruption Data to ITER. W70 7/10/09 8/24

WTKM explained the toroidal asymmetry in Ipl on JET

Hiro current theory has amazing consistency with experiment in the sign of the effect and its time dependence. No tricks are necessary.

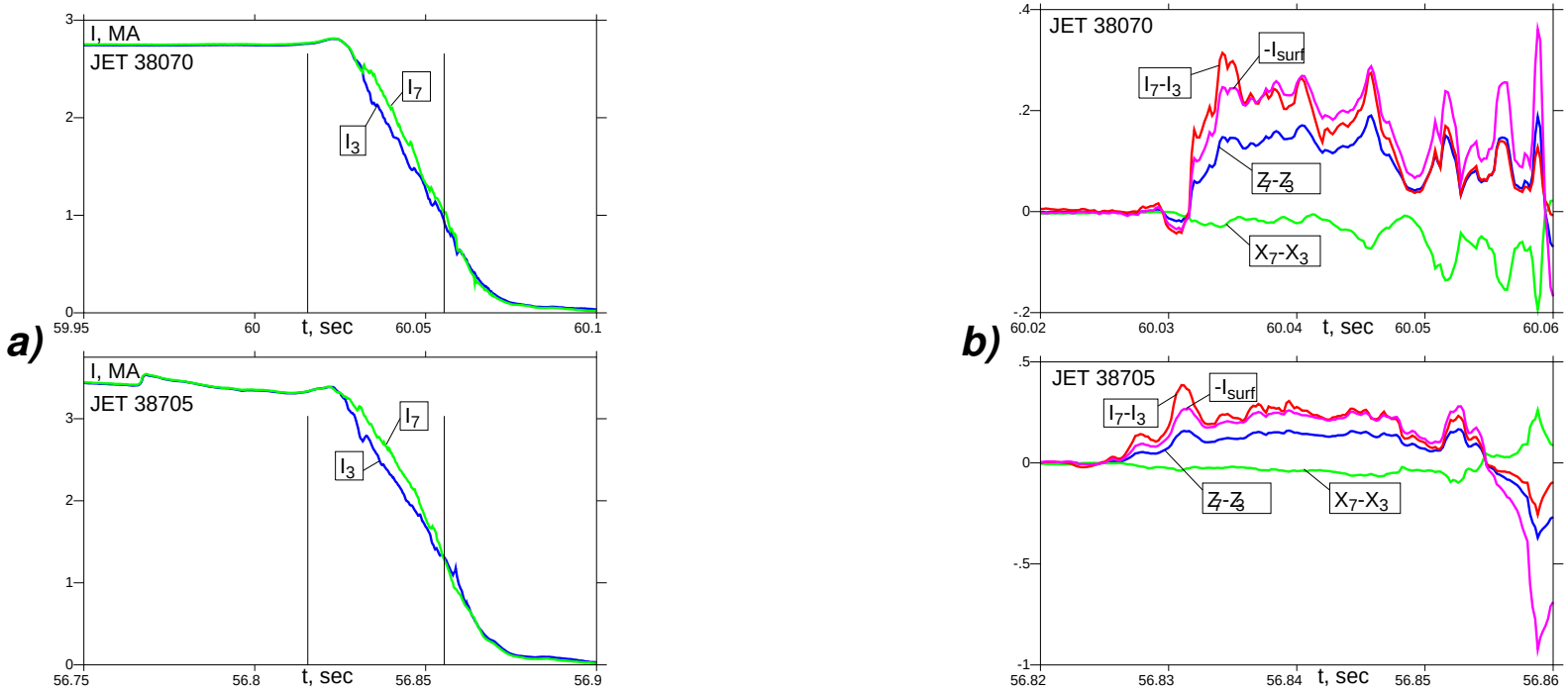

(a) Plasma currents $I_{3,7}$ in octants 3,7 on JET during the disruptions.
(b) $Z_7 - Z_3$ and $R_7 - R_3$, $I_7 - I_3$ and its prediction $-I^{surf}$ from the present theory.

$$I_{est}^{surf} \simeq -a\frac{4B_\varphi}{R_0\mu_0}\frac{\delta Z_{7,3}}{2} \ll I^{surf}, \quad Z_{7,3} \equiv \frac{1}{\mu_0 I_{pl}}\oint fB\tau dl \simeq \frac{1}{2}z_{p,7,3},$$
$$\mu_0\vec{\imath}_{11} = -2\xi_{11}\frac{B_\varphi}{R}\left(\mathrm{e}_\varphi + \frac{a}{R}\mathrm{e}_\theta\right), \quad I_{Hiro} \simeq I_{surf} = -4a\xi_{11}\frac{B_\varphi}{R\mu_0}. \tag{3.1}$$

Hiro currents explain toroidal asymmetry in Ipl

100 % success in explanation of the sign of toroidal asymmetry on wall currents on JET

(in contrast to 100 % failure of "halo current"interpretations)

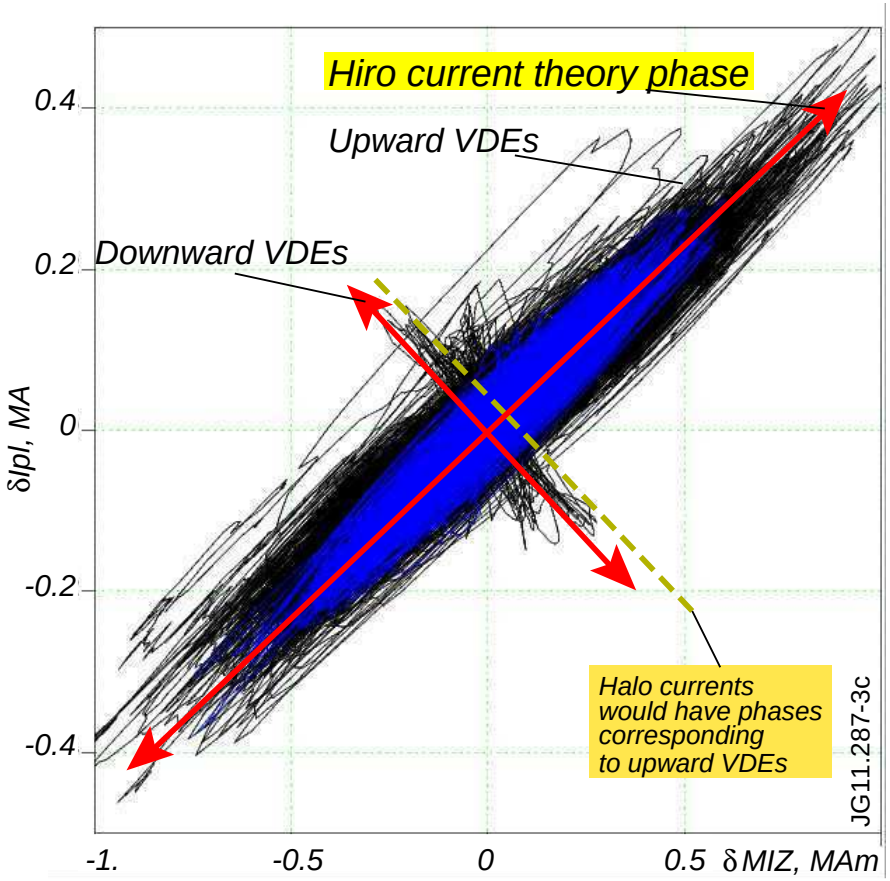

dB (Aug. 2014) for the Phase diagram

PSC	Octants	All cases	VDE
C-wall	3-7	4429	1673
C-wall	1-5	963	299
IL-wall	3-7	371	162
IL-wall	1-5	391	160

Vertical axis

$$\delta I_{pl} \equiv I_{pl}(\varphi+\pi,t) - I_{pl}(\varphi,t)$$

Horizontal axis:

$$\delta M_{IZ} \equiv M_{IZ}(\varphi+\pi,t) - M_{IZ}(\varphi,t)$$

Black color: $\varphi = 90^o$ **for Octants 7-3**
Blue color: $\varphi = 0^o$ **for Octants 1-5**

The currents in the wall measured on JET are the Hiro currents

3.2 JET asymmetry in the Diamagnetic signal

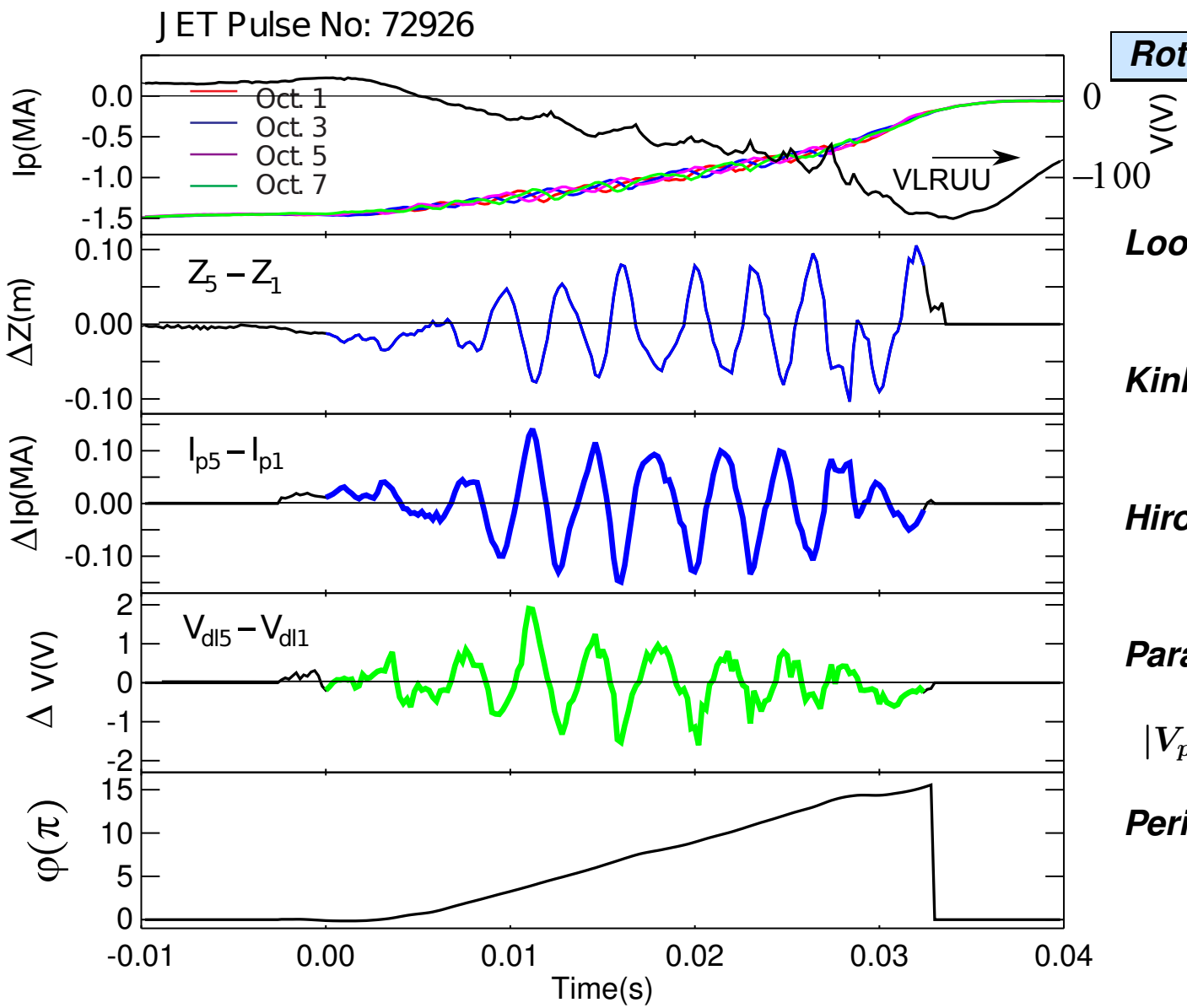

Rotating m/n=1/1 WTKM

Loop Voltage

$$U \simeq -50\ V$$

Kink 1/1 amplitude

$$\xi \simeq 5\ cm$$

Hiro currents

$$I^{Hiro} \simeq 0.2\ MA$$

Paramagnetic Voltage

$$|V_{pol}| = \left| -\frac{d\Phi_{tor}}{dt} \right| \simeq 1\ V$$

Period of rotation

$$\Delta t \simeq 3\ ms$$

Paramagnetic Voltage on Diamagnetic loop is consistent with the local enhancement of Evans currents !!!

"Locked" m/n=1/1 WTKM on JET (Gerasimov 2014)

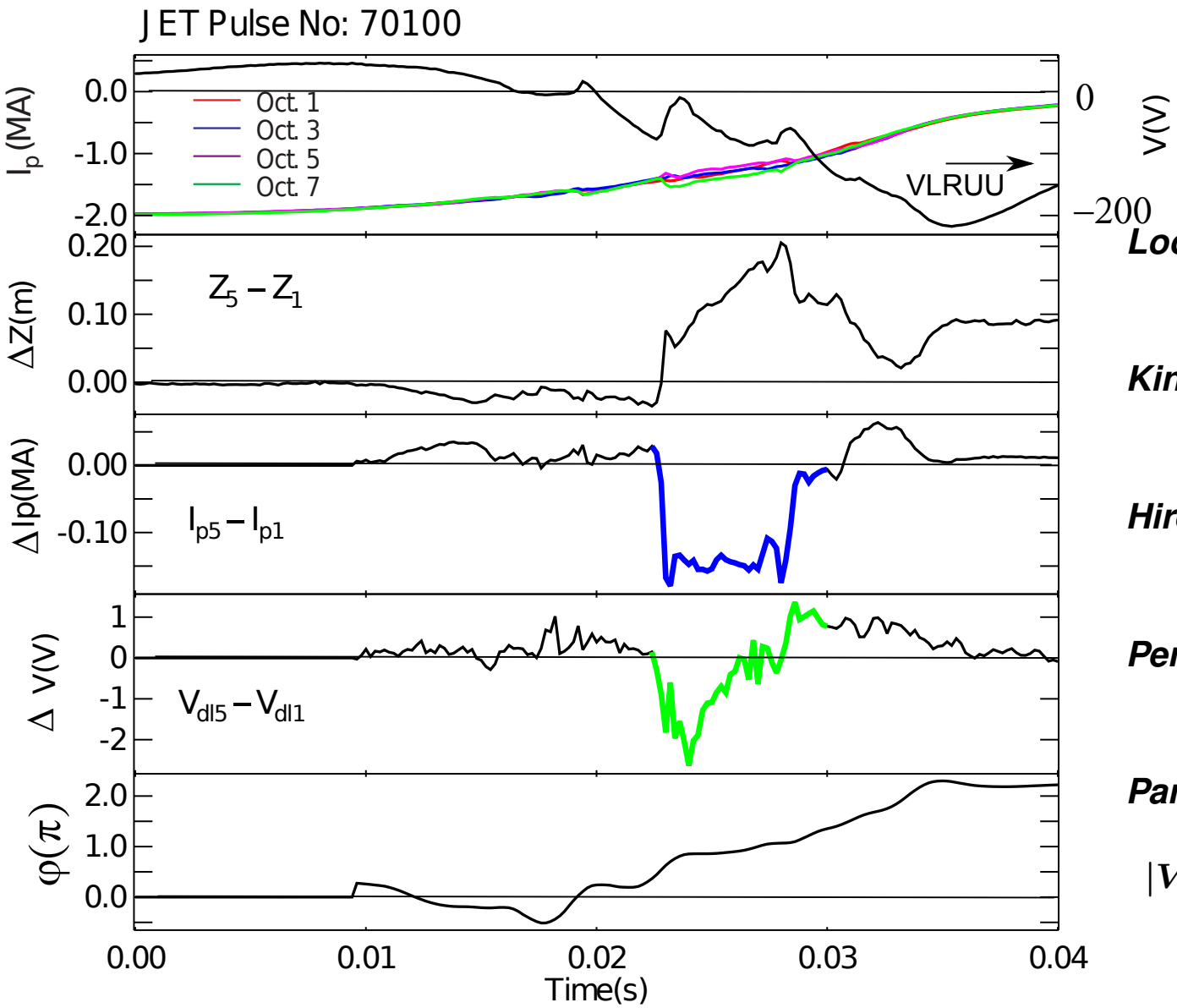

Loop Voltage

$$U \simeq -70\ V$$

Kink 1/1 amplitude

$$\xi \simeq 8\ cm$$

Hiro currents

$$I^{Hiro} \simeq 0.15\ MA$$

Period of rotation

$$\Delta t \simeq 25\ ms$$

Paramagnetic Voltage

$$|V_{pol}| = \left| -\frac{d\Phi_{tor}}{dt} \right| < 2\ V$$

Paramagnetic Voltage on Diamagnetic loop is consistent with the local enhancement of Evans currents !!!

The theory interpretation of $\delta\dot{\Phi}$ asymmetry

1. *The halo-zone is toroidally localized in the vicinity of the wetting zone*
2. *Both Hiro and Evans currents enter the wall structure (Hiro currents escape magnetic probes)*
3. *The Hiro currents are situated right after the plasma core edge which have the same Φ in all cross-sections*
4. *The Evans currents have a larger footprint and generate an extra paramagnetic flux*

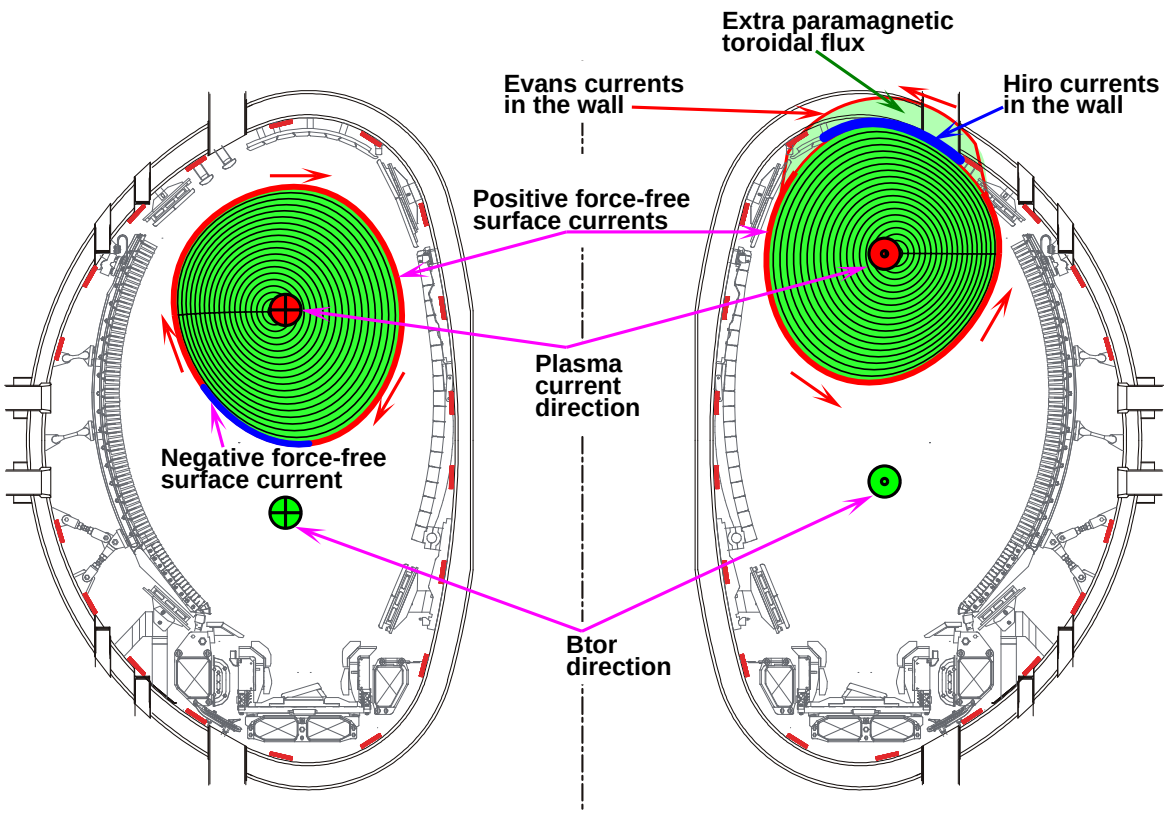

Theory suggests that Evans currents in the wetting zone are responsible for asymmetry in $\delta\Phi$

The relevant reference numbers used

$< n_e >$	$3 \cdot 10^{19}$	- average core plasma density
V_{olume}	60 m^3	- plasma volume
t^{CQ}	$\simeq 25$ ms	- current quench time for assessment of $\dot{N}_e$
$Q = 2en_eV_{olume}$	600 A·s	- total particle charge

The reference limit on the Evans current

$$I^{Evans} \leq 2e\frac{dN}{dt} = \frac{600}{0.025} \simeq 0.024\ MA. \tag{3.2}$$

For explanation of the $\delta\Phi$ asymmetry it is necessary to have

$$\mu_0 \frac{I^{Evans}}{L^{wet}} = \delta B_{tor} = \frac{\delta\Phi}{\delta S^{Evans}}. \tag{3.3}$$

For rotating mode 72926 it is OK

$$\begin{aligned} I^{Evans}_{MA} &\simeq \frac{V_{pol}\Delta t}{2\pi\mu_0\delta S^{Evans}} L^{wet} \\ &\simeq 0.01 \cdot \frac{0.2}{\delta S^{Evans}_{m^2}} \cdot \frac{L^{wet}_m}{5} \end{aligned} \tag{3.4}$$

For the locked mode 70100 it seems to be too large

$$I^{Evans}_{MA} \simeq \frac{\int V_{pol}dt}{\mu_0\delta S^{Evans}} L^{wet} \qquad \simeq 0.25 \cdot \frac{0.2}{\delta S^{Evans}_{m^2}} \cdot \frac{L^{wet}_m}{5} \tag{3.5}$$

They may have reached the saturation level causing the drop in $\delta\dot{\Phi}$

Hiro currents in Large disruption shot 38070

For 38070 VDE the measured charge carried by the Hiro currents on JET is calculated as

$$\int (I_7 - I_3)_{38070} dt = \int I_{38070}^{Hiro} dt = 4350\ [A \cdot s] \gg 600 \tag{3.6}$$

The electric charge of the shadow plasma is approximately two orders of magnitude smaller than 600 As.

The physics of the Hiro currents is not associated with the "halo"currents (limited by the total charge)

Although it is impossible to affect the misuse of "halo"current term in this community, the "halo"-name is highly confusing and works against the progress (and in certain cases in PPP is an assault on the authors of the theory)

4 Tokamak MHD (TMHD)

Typical conventiona MHD:

Equation of motion

$$\rho\frac{d\vec{V}}{dt} = -\nabla p + (\vec{\jmath}\times\vec{B}) + \textbf{(hyper-) viscosity.} \tag{4.1}$$

Equation of state

$$\frac{dp}{dt} = -\gamma p(\nabla\cdot\vec{V}), \quad \frac{d\rho}{dt} = -\rho(\nabla\cdot\vec{V}). \tag{4.2}$$

Ampere's law

$$\vec{B} = (\nabla\times\vec{A}), \quad \mu_0\vec{\jmath} = (\nabla\times\vec{B}). \tag{4.3}$$

Faraday's law

$$-\frac{\partial\vec{A}}{\partial t} + (\vec{V}\times\vec{B}) - \nabla\phi^E = \frac{\vec{\jmath}}{\sigma}, \quad \sigma = \sigma(T_e). \tag{4.4}$$

Boundary conditions

$$\begin{aligned} &(\vec{E}\times\vec{n})_{plasma} = (\vec{E}\times\vec{n})_{wall} \quad \textbf{from electrodynamics,} \\ &\vec{V}_\perp = (\vec{V}\cdot\vec{n})_{wall} = 0 \qquad \textbf{from hydrodynamics.} \end{aligned} \tag{4.5}$$

Three levels of MHD

1. ***Hydrodynamics and MHD of liquid metals. Inertia is important.***
2. ***3-D numerical plasma codes (with a train of equation irrelevant to MHD)***
3. ***Tokamak MHD - highly anisotropic plasma with negligible inertia.***

The distance between first two is smaller than between the second and the third.

Force balance versus plasma inertia in disruptions

Discharge parameters of 38070:

n_e	$\simeq 3 \cdot 10^{19}$	***plasma density***
V_{olume}	$\simeq 50$ ***m***^{3}	***plasma volume***
ξ	< 0.3 ***m***	***amplitude of the m/n=1/1 perturbation***
Δt	***25 ms***	***duration of m/n=1/1 perturbation***

Force of plasma inertia

$$F_a \simeq m_i n_i \cdot V_{olume} \cdot \frac{2\xi}{(\Delta t)^2} \quad \simeq 2 \cdot 1.7 \cdot 10^{-27} \cdot 3 \cdot 10^{19} \cdot 50 \cdot \frac{0.6}{625 \cdot 10^{-6}} \qquad (4.6)$$
$$\simeq 0.005\ [N].$$

The measured value of the sideways force in this shot is

$$\boxed{\simeq 2.4\ MN = 2.4 \cdot 10^6\ N \gg 0.005\ N}$$

- ***All existing 3-D codes are driven by plasma inertia, negligible in tokamaks.***

The mismatch between 3-D code models and the tokamak reality is 10^8 in driving forces or 10^4 in the time scale

- ***Some of 3-D codes (M3D) are dare to claim that they simulate disruptions and the sideways force in ITER. To operate, they need an artificially strong instability.***

  The trick M3D uses is a hidden enhancement of ITER 15 MA current to the level of 24 MA, not reflected in the title, abstract, introduction, summary and in presentations

The set of TMHD equations

The Tokamak MHD is presented by the following set of equations

1. *Equation of motion is split into an equilibrium equation*

$$\nabla p = (\vec{\jmath} \times \vec{B}), \quad \bar{\Psi} = \bar{\Psi}(\bar{\Phi}), \tag{4.7}$$

and the plasma boundary advancing equation

$$\lambda \vec{\xi} = -\frac{\bar{F}}{r^2}\nabla \tilde{F}, \quad \left(\nabla \cdot \frac{\bar{F}^2}{r^4}\nabla \tilde{F}\right) = 0. \tag{4.8}$$

2. *Faraday's (Ohm's) law in plasma and the wall (with no $\vec{V}$)*

$$-\frac{\partial \vec{A}}{\partial t} - \nabla \varphi^E + (\vec{V} \times \vec{B}) = \frac{\vec{\jmath}}{\sigma}, \quad \vec{V} \equiv \frac{d\vec{\xi}}{dt}. \tag{4.9}$$

3. *Plasma anisotropy*

$$\sigma = \sigma(\bar{\Phi}), \quad (\vec{B} \cdot \nabla) \simeq 0. \tag{4.10}$$

4. *boundary condition at the wall (determines plasma V_{normal} to the wall)*

$$\vec{E}_{\parallel}^{pl} = \vec{E}_{\parallel}^{wall} = \frac{\vec{\jmath}^{pl}}{\sigma^{pl}} - (\vec{V} \times \vec{B}) = \frac{\vec{\jmath}^{wall}}{\sigma^{wall}}. \tag{4.11}$$

Force balance across the free plasma surface

$$\left(p + \frac{|\vec{B}|^2}{2\mu_0} + \frac{\bar{F}\tilde{F}}{r^2\mu_0}\right)_i = \left(\frac{|\vec{B}|^2}{2\mu_0}\right)_e, \tag{4.12}$$

where subscripts 'i, e' specify the inner and outer sides of the plasma surface.

The numerical scheme of TMHD is simply beautiful

Each of all TMHD equations has its own energy principle leading to a positively defined symmetric matrix if expressed in terms of finite elements. Stability is guarantied

3-D equilibrium (3-D Hermit elements, block tri-diagonal)

$$
\begin{aligned}
W^{\vec{j}\times\vec{B}} \equiv & \frac{1}{2}\int\left(\frac{|\vec{B}|^2}{2\mu_0}-(\vec{A}\cdot\vec{j})\right)d^3\mathrm{r} \\
\equiv & \frac{1}{2\mu_0}\int\Big\{K(\bar{\Psi}'+\psi'_a+\bar{\Phi}'\eta'_\zeta)^2-2N(\bar{\Psi}'+\psi'_a+\bar{\Phi}'\eta'_\zeta)(\psi'_\theta-\phi'_\zeta)+M(\psi'_\theta-\phi'_\zeta)^2 \\
& +Q(\bar{\Phi}'+\phi'_a+\bar{\Phi}'\eta'_\theta)^2-2\tilde{N}(\bar{\Psi}'+\psi'_a+\bar{\Phi}'\eta'_\zeta)(\bar{\Phi}'+\phi'_a+\bar{\Phi}'\eta'_\theta) \\
& +2\tilde{M}(\psi'_\theta-\phi'_\zeta)(\bar{\Phi}'+\phi'_a+\bar{\Phi}'\eta'_\theta)-(\bar{\Phi}+\phi)\hat{F}'_a+(\bar{\Psi}+\psi)(\hat{J}'_a+\nu'_\theta)\Big\}\,da\,d\theta\,d\zeta.
\end{aligned}
\tag{4.13}
$$

Plasma advancing (3-D Hermit elements, block tri-diagonal)

$$
W^F=\frac{1}{2}\int\bar{F}^2\frac{g^{aa}\tilde{F}'^2_a+2g^{a\theta}\tilde{F}'_a\tilde{F}'_\theta+g^{\theta\theta}\tilde{F}'^2_\theta+2g^{a\zeta}\tilde{F}'_a\tilde{F}'_\zeta+2g^{\theta\zeta}\tilde{F}'_\theta\tilde{F}'_\zeta+g^{\zeta\zeta}\tilde{F}'^2_\zeta}{r^4}J\,da\,d\theta\,d\zeta. \tag{4.14}
$$

Faraday's law (3-D Hermit elements, block tri-diagonal)

$$
W^t=\frac{1}{2}\int\left\{\frac{\partial}{\partial t}\left(KB^\theta B^\theta+2\tilde{M}B^\theta B^\zeta+QB^\zeta B^\zeta\right)+\eta^{pl}\left(Kj^\theta j^\theta+2\tilde{M}j^\theta j^\zeta+Qj^\zeta j^\zeta\right)\right\}d^3r. \tag{4.15}
$$

Sink/source wall current from the plasma (triangle based wall model, small sparse matrix)

$$
W^S=\int\left\{\frac{\bar{\sigma}(\nabla\phi^S)^2}{2}+j_\perp\phi^S\right\}dS-\frac{1}{2}\oint\phi^S\bar{\sigma}[(\vec{n}\times\nabla\phi^S)\cdot d\vec{l}]. \tag{4.16}
$$

Hiro, eddy currents in the wall (triangle based wall model, stationary matrix)

$$
W^I\equiv\frac{1}{2}\int\left\{\frac{\partial(\vec{\imath}\cdot\vec{A}^I)}{\partial t}+\bar{\eta}|\nabla I|^2+2\left(\vec{\imath}\cdot\frac{\partial\vec{A}^{ext}}{\partial t}\right)\right\}dS-\oint(\phi^E-\phi^S)\frac{\partial I}{\partial l}dl. \tag{4.17}
$$

5 The VDE-code for EAST to be a research tool

Real EAST in-vessel geometry is used for VDE simulations.

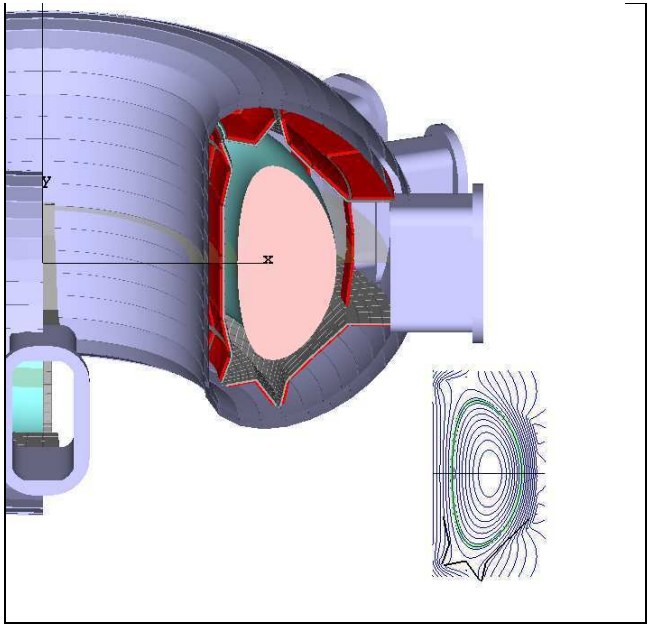

Initial unstable plasma

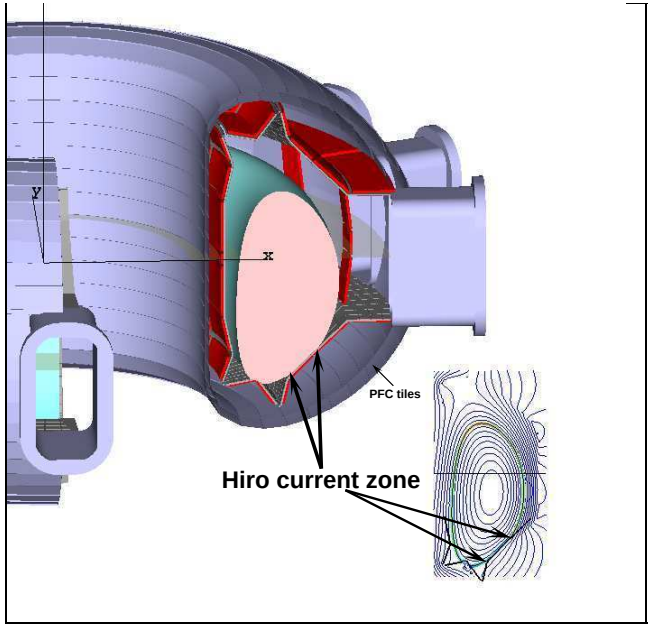

Plasma touches the divertor plate and generate Hiro currents, $\Phi/\Phi_0 = 1$

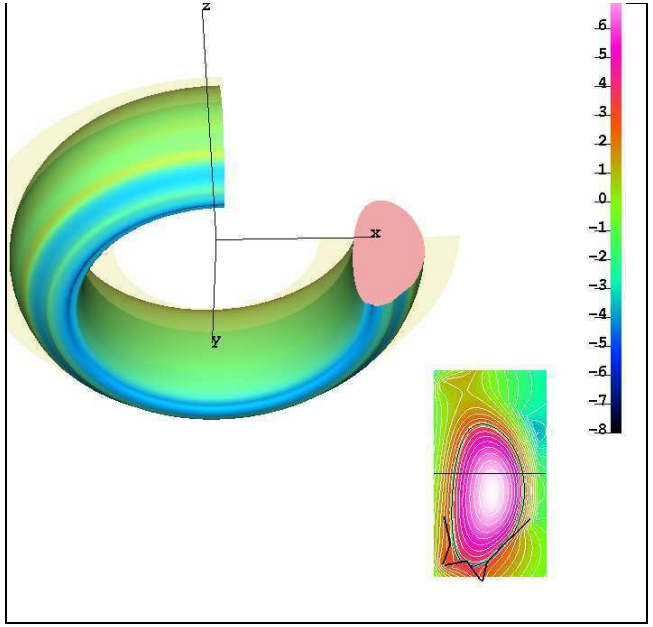

Negative Hiro currents (blue), shown in the contact area of plasma

!!! Our VDE code shows the contact zone right at the position of Xiong tiles !!!

Plasma VDE in EAST geometry

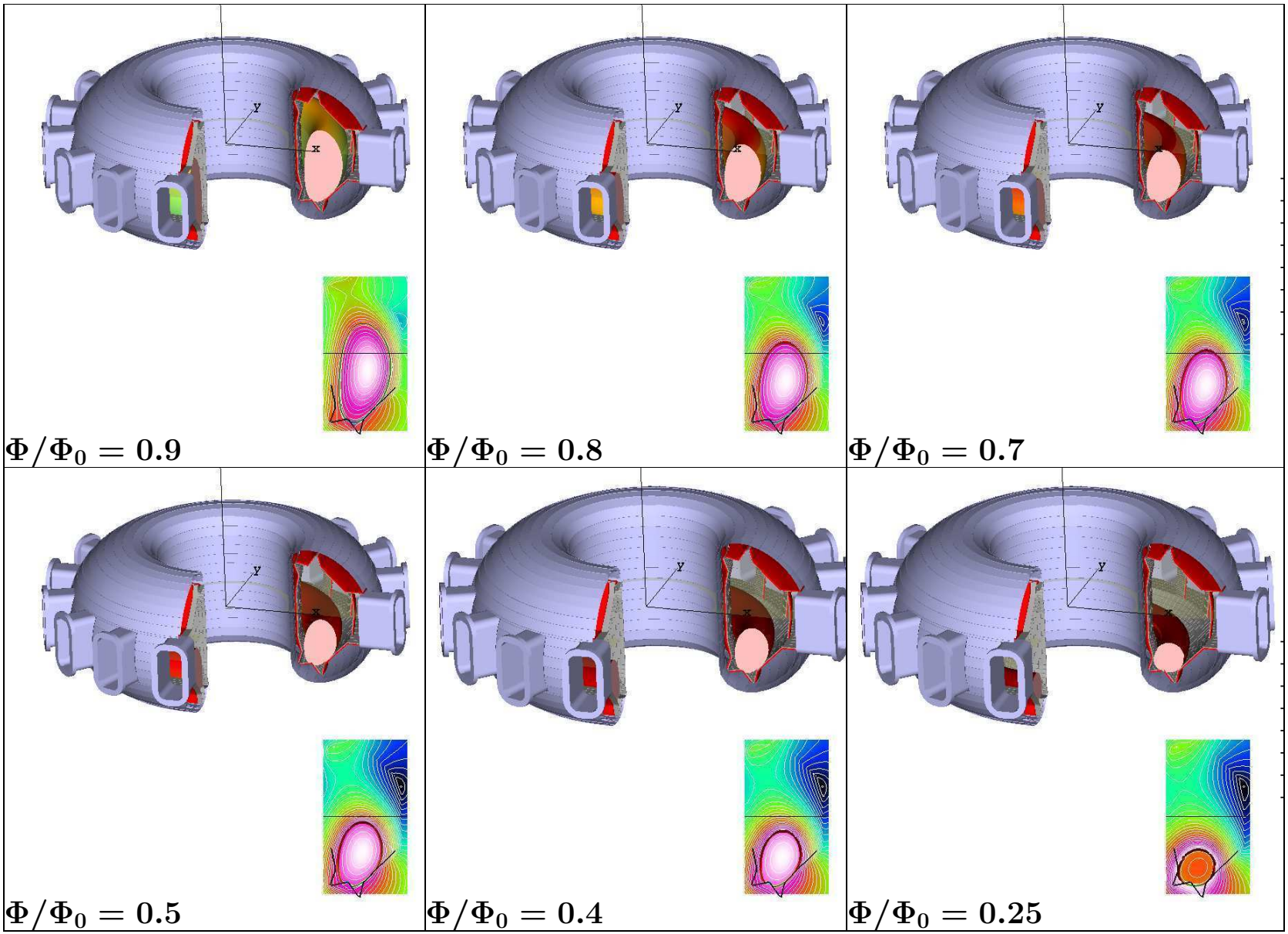

5.1 The real in-vessel geometry is an essential part

Real EAST in-vessel geometry is used for VDE simulations.

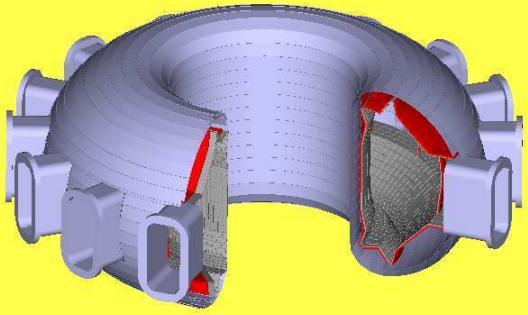

Vacuum Chamber

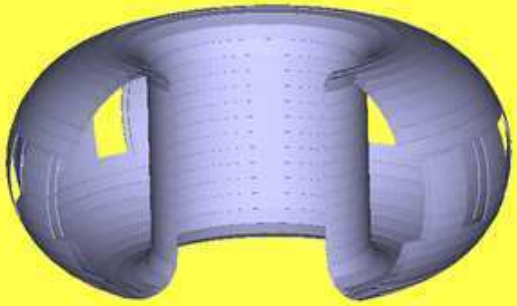

Double layer vacuum vessel

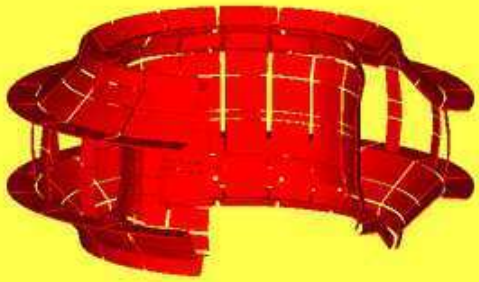

Stabilizer elements (16 toroidal sections)

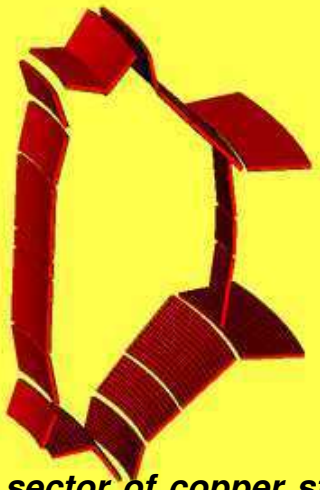

One toroidal sector of copper stabilizers (8728 triangles)

All associated Greens functions for wall circuit equations are already calculated

Only

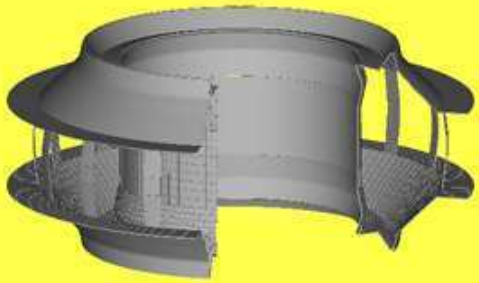

Carbon plasma facing tiles

5.2 Free-boundary equilibria with ESC-EEC

ESC-EEC can calculate free-boundary equilibria in both $r - z$ and flux coordinates

The Equilibrium Spline Interface (ESI) is developed for equilibrium codes instead of present mess in interfacing

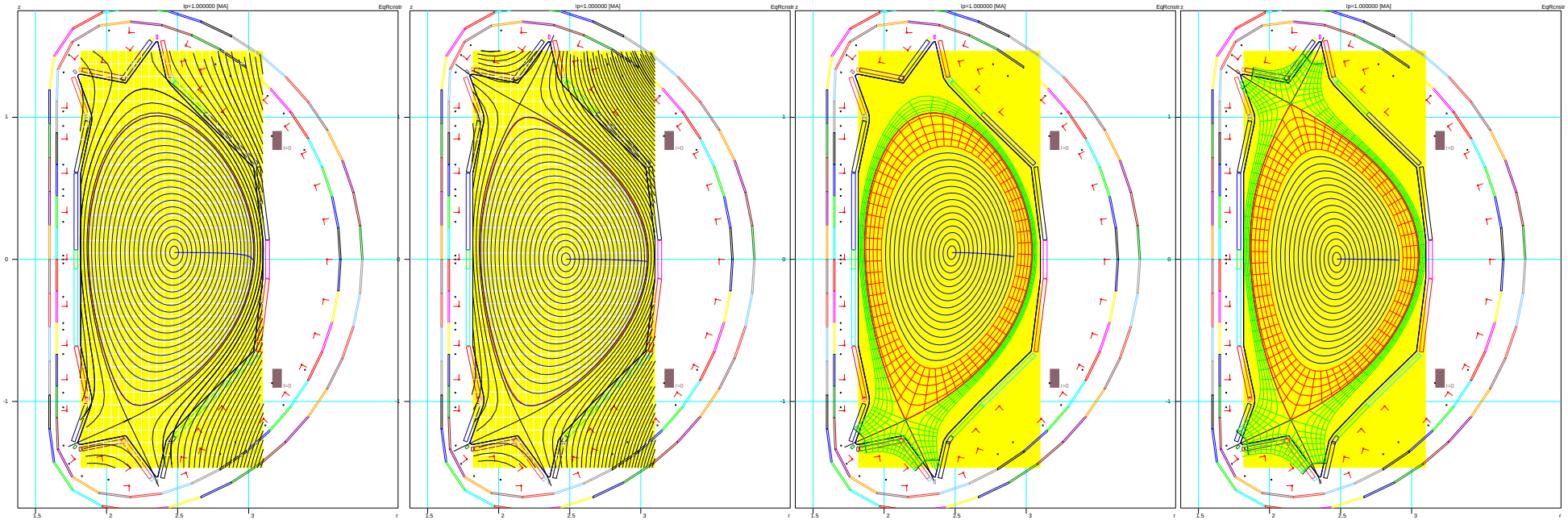

(a) ID=00,1,00,00,00 (b) ID=00,01,00,00,00 (c) ID=00,40,00,00,23 (d) ID=00,40,00,00,23

Free boundary ESC-EEC is a step for inclusion of going beyond δ-functional TMHD toward development of the physics of the Evans currents in the halo-zone

5.3 VDE simulations motivate innovative diagnostics

We suggested a comprehensive set of innovative tile diagnostics for Hiro, Evans and SoL current measurements on NSTX-U

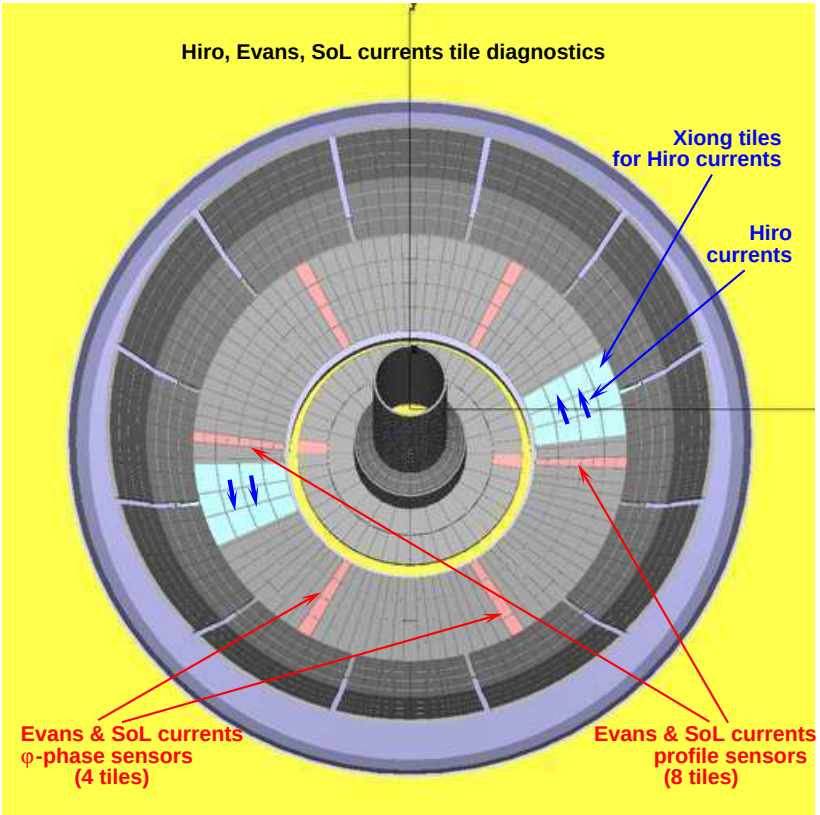

Tile sensors for measuring Hiro, Evans, and SoL currents and different kinds of diagnostics including

1. ***Hiro current diagnostics***
2. ***Evans current profile diagnostics with enhanced radial resolution***
3. ***Evans current φ-phase diagnostics***
4. ***SoL current measurements***

Evans currents carry important information on plasma-PFC interactions, never touched

TMHD vs existing MHD simulations

Regarding disruptions, everything is either wrong or highly irrational in theory and existing 3-D simulations

	The current "Flagship" 3-D MHD codes	*TMHD (VDE, Galkin's DSC codes)*
1	*Wrong interpretation of the Eq. of motion*	*Proper extraction of the force balance*
2	*Unresolvable, 4 decades old Courant time step limit problem*	*Just absent*
3	*It is a non-sense to solve the eq. equation using inertia*	*Fast, stable Newton scheme, tested in 2-D*
4	*Numerical plasma grid misaligned with magnetic field*	*Adaptive Reference Magetic Coordinates*
5	*Inability to implement* $(\vec{B} \cdot \nabla\sigma) \simeq 0$ *(Lundquist problem)*	*Consistency with the scale separation*
6	*Associated train of irrelevant "extended MHD" equations*	*Compact with nothing unnecessary*
7	*Simplistic wall geometry*	*3-D, triangle based thin wall surface*
8	*Rare plasma with Spitzer resistivity outside the plasma edge*	*Vacuum,* $\sigma = 0$
8	*Wrong, "salt-water" condition at PFC* $V_{normal}^{plasma} = 0$	*Plasma neutralization*
9	*Unstructured triangle based numerical grid (intrinsically C-0) for plasma and*	*Hermite C-1 elements and block-diagonal matrixes*
10	*Unjustified use of C-1 triangles, misaligned with* $\vec{B}$	*Aligned with* $\vec{B}$ *and are C-1 automatically*
11	*Crowds of people for serving a single the non-operational code*	*CodeBuilder, a physicist, Chinese student, the Head of JET magnetics, & S.Galkin*
12	...	...

For more than 3.5 decades since the late 1970s the 3-D codes have generated countless "disruption" simulations

In 1996, JET disruption data and the WTKM theory in 2007 have devaluated them all together (with the exception of A.Aydemir's code)

6 Summary

1. ***TMHD created a credible, predictive theory of the VDE in tokamaks, consistent with observatons and extendable to more details in physics***
2. ***New set of MHD equations, compact and rational, is derived for VDE***
3. ***New stable and fast numerical are formulated for implementation***
4. ***2-D version of the VDE code is operational and on the way to be a research tool for the EAST tokamak.***
5. ***New tile diagnostics are motivated for tokamak disruptions***

This prepare a transition to further progress in disruption understanding, which will require the close cooperation of theory, numerical simulations and experimental measurements and interpretations

The major concern at the moment is that the potentially big effect of the Hiro currents on the Be plasma facing tiles in ITER is being neglected in its disruption analysis